HOSTED BY

ELSEVIER

Contents lists available at ScienceDirect

Saudi Journal of Biological Sciences

journal homepage: www.sciencedirect.com

الجمعية السعودية لعلوم الحياة
SAUDI BIOLOGICAL SOCIETY

Original article

Valorizing pomegranate wastes by producing functional silver nanoparticles with antioxidant, anticancer, antiviral, and antimicrobial activities and its potential in food preservation

Asmaa Ali Alharbi [a,*], Amira M. Alghamdi [a], Soha Talal Al-Goul [b], Aminah Allohibi [c], Roua S. Baty [d], Safa H. Qahl [e], Eman A. Beyari [f]

[a] Department of Biochemistry, Faculty of Science, King Abdulaziz University, Jeddah 21589, Saudi Arabia
[b] Department of Chemistry, College of Sciences & Arts, King Abdulaziz University, Rabigh 21911, Saudi Arabia
[c] Biological Sciences Department, College of Science & Arts, King Abdulaziz University, Rabigh 21911, Saudi Arabia
[d] Department of Biotechnology, College of Science, Taif University, PO Box 11099, Taif 21944, Saudi Arabia
[e] Department of Biological Science, College of Science, University of Jeddah, P.O. Box 80327, Jeddah 21589, Saudi Arabia
[f] Department of Biological Sciences, Microbiology, Faculty of Science, King Abdulaziz University, Jeddah 21589, Saudi Arabia

ARTICLE INFO

Keywords:
Antioxidant
Anticancer
Food preservation
Pomegranate waste
Silver nanoparticles
Toxicity

ABSTRACT

The food sector generates massive amounts of waste, which are rich in active compounds, especially polyphenols; therefore, valorizing these wastes is a global trend. In this study, we produce silver nanoparticles from pomegranate wastes, characterized by enhanced antioxidant, anticancer, antiviral, and antimicrobial properties and investigated their potential to maintain the fruit quality for sixty days in market. The pomegranate waste-mediated silver nanoparticles (PPAgNPs) were spherical shape (measured by TEM), 20 nm (Zeta sizer), negatively charged −25.98 mV (Zeta potential), and surrounded by active groups (FTIR). The PPAgNPs scavenged 94 % of DPPH radicals and inhibited the growth of pathogens, i.e., *Staphylococcus aureus, Listeria monocytogenes, Campylobacter jejuni, Salmonella typhi* and *Candida* with inhibition zones diameters (16–45 mm). They impeded the development of breast and colon cancer cell lines by 80 and 78 %, increased the activity of apoptosis marker caspase 3, and inhibited 82 % of COVID-19. The PPAgNPs were added to the rat diet at 80, 160, and 320 μg/kg levels. PPAgNPs administered at a concentration of 160 μg/kg in the rat diet resulted in the best growth performance, normal liver and kidney parameters ($p = 0.029–0.038$), lowered lipid profile, malondialdhyde (MDA), and raised glutathion reduced (GSH), total protein (TP). Also, the reduced gene expression of Interleukin 6 (IL-6) and Tumor necrosis factor alpha (TNF-α) in albino rats' serum indicates the anti-inflammatory effect of PPAgNPs. PPAgNPs developed a functional coating to preserve mandarin fruit for 60 days by dipping technique. The active coat containing PPAgNPs can effectively preserve the fruit for 60 days.

1. Introduction

The natural compounds from plant and microorganisms play an essential role in the bio-fabrication of nanoparticles as a reducing agent (El-Ashry et al., 2022; Khairy et al., 2022; Yehia et al., 2022). In this study, we fabricated silver nanoparticles from pomegranate juice processing waste; *Punica granatum* belongs to the Iranian-native Punicaceae family and the Himalayas in India; its fruit is consumed worldwide in producing juices and beverages 322 to 341 L of juice were produced after the processing of one tonne of pomegranate fruits are produced along with almost 669 kg of pericarp, rinds, and peels, which accounts 50 % (Hasnaoui et al., 2014). Processing byproducts from pomegranate juice include the seeds, outer peels (husks), rind membranes, and piths of the fruit; these wastes are rich in bioactive components and, therefore, have various activities antiviral, antimicrobial, anticancer, and antioxidant properties (Ko et al., 2021). Thus, this study converted pomegranate biowastes with potential into value-added products as green silver nanoparticles.

Peer review under responsibility of King Saud University.
* Corresponding author.
E-mail addresses: aanalharbi@kau.edu.sa (A. Ali Alharbi), Amaalghamdi1@kau.edu.sa (A.M. Alghamdi), salgoul@kau.edu.sa (S. Talal Al-Goul), mallehabi@kau.edu.sa (A. Allohibi), rsbaty@tu.edu.sa (R.S. Baty), shqahal@uj.edu.sa (S.H. Qahl), Eboyari@kau.edu.sa (E.A. Beyari).

https://doi.org/10.1016/j.sjbs.2023.103880
Received 15 October 2023; Received in revised form 8 November 2023; Accepted 24 November 2023
Available online 25 November 2023

Silver nanoparticles are frequently employed in biomedical applications, research, solar cells, water purification systems, and optoelectronics because of their unique qualities (El-Saadony et al., 2019; Sabra et al., 2022). Their potential for usage in biomedicine is significantly constrained by the utilization of expensive, unstable, and poisonous chemicals (Alagawany et al., 2021; El-Saadony et al., 2021; Mawed et al., 2022). Therefore, biological methods remain the best, including medicinal plant extracts, fungi, and prokaryotic bacteria employed for the green synthesis of AgNPs because of its time-saving, cost-effective, and environmentally benign procedure vs chemical and physical techniques (Mazen et al., 2017).

Nanomaterials are helpful in many disciplines, including medical, because of their small size and high reactive surface to volume ratio (Abdel-Raouf et al., 2017). Because of their distinctive chemical, biological, and physical features, silver nanoparticles (AgNPs) are essential. The bio-reduction process has no adverse effects on its applications (Dutta et al., 2020).

Green-synthesized AgNPs are highly effective cytotoxic and antibacterial agents due to their size and shape (Gherasim et al., 2020). Many studies stated that green silver nanoparticles have great potential against MDR bacteria and fungi, inhibiting cancer growth and inflammation (Saad et al., 2021a; Alowaiesh et al., 2023). AgNPs and other nanoparticles have been studied in the post-antibiotic era to find new agents that can fight diseases without promoting the establishment of new resistances (Betts et al., 2018). As infections resulting from microorganisms resistant to antibiotics are a worldwide issue, AgNPs are an attractive substitute for preventing diseases cleaning medical equipment, and even battling diseases that are caused by these microorganisms (Natan and Banin, 2017). Numerous findings have shown the exceptional antitumor activity of sustainable silver nanoparticles, which can passively and actively target cancerous tissue (Kovács et al., 2022); besides, silver nanoparticles can directly act on viruses, and on their first steps of interaction with the host cell, depending on several factors, such as size, shape, functionalization and concentration.

Massive losses in fresh postharvest crops reduce their export values and foreign exchange. Citrus fruits are famous worldwide due to the abundance of bioactive compounds (Forner-Giner et al., 2023); however, prolonged cold storage affects the performance of these beneficial substances, leading to food loss (Ehlers, 2016). Like citrus, Mandarin fruit has a long shelf life after harvest but is susceptible to rind physiological abnormalities and deterioration due to microbial infections, causing economic losses (Zacarias et al., 2020).

The standard control of postharvest disorders depends on using chemical fungicides, i.e., imazalil and thiabendazole, that adversely impact the health and environment (Chavan et al., 2023). Therefore, commercial waxes such as oxidized polyethylene effectively prevented water loss and gas exchange in citrus, maintaining fruit quality (Yadav et al., 2022; Chavan et al., 2023). Usually, these waxes were a carrier for synthetic fungicides; consequently, they were prohibited globally due to their harmful impacts on environmental and human health (Chowdhury et al., 2022). Edible natural coatings are the alternatives for synthetic waxes, i.e., gum arabic, carnauba wax, chitosan, carboxymethyl cellulose, and beeswax (Bhan et al., 2022).

Arabic gum is a polysaccharide, a carrier for essential elements, containing a dense network of hydrogen bonds, resulting in excellent O_2 and CO_2 barrier qualities (Manzoor et al., 2022). It can be used as a vehicle for antioxidants, antibacterial agents, and flavors, which are crucial for sustaining the quality of horticulture crops such as mandarins. However, it has been noted that Arabic gum has weak water vapor barrier characteristics (Bhan et al., 2022; Chavan et al., 2023); therefore, the need to strengthen it with antibacterial inorganic materials, i.e., zinc oxide, magnesium oxide, and silver nitrate, were incorporated in edible coating formulations; Silver being an excellent antimicrobial agent, also been applied to food packaging (Ahmad et al., 2021).

Because of the poor stability of these materials in the Coating, they were replaced with nanomaterials, especially green synthesized nanoparticles, to create a bio-nanocomposite polymer to improve packed foods' shelf life (Jafarzadeh et al., 2023). According to Wang et al., (2022), nanomaterials have been reported to improve the edible coating polymer matrix's functional properties, structure, and steadiness. Regarding, Simbine et al., (2019) applied Ag-nanoparticles in food packages and noted that AgNPs should be produced by ecologically correct methods; also, Srikhao et al., (2022) found that paper coated with silver nanoparticles is effective in killing bacteria and viruses. Therefore, it can be included in different packages.

Numerous findings have investigated using Arabic gum as a fruit coating material. However, including PPAgNPs in Arabic gum coatings to improve their properties has not been thoroughly utilized. There are no previous studies about the effects of the postharvest application of PPAgNPs in an AG complex on the lifetime and quality of Vermont mandarins. Therefore, in this study, we characterized the PPAgNPs with different devices, evaluated the phenolic profile of AgNPs compared to pomegranate waste extract, evaluated biological effects, including anti-inflammatory, antibacterial, and anticancer, and then assessed the safety of green silver nanoparticles on albino rats, the effectiveness of AgNPs in an AG coating in retaining the quality features of Vermont mandarin fruit was examined. This approach may assist in preserving the storage quality of Vermont mandarins.

2. Materials and methods

2.1. Pomegranate waste extract preparation (PWE)

Pomegranate waste was collected, washed with tap water, dried in the oven, and then powdered. A 50 g of pomegranate waste powder were homogenized in 300 mL of distilled water and then heated at 50 °C for 45 min to obtain pomegranate waste extract (PWE). The PWE was stored at 4 °C in the refrigerator (Alowaiesh et al., 2023). Scheme 1 show the expermental layout of biological activity of AgNPs and its applications.

2.2. Green preparation of silver nanoparticles

Silver nitrate ($AgNO_3$) was acquired from Sigma Aldrich and employed as a precursor. 5 mL of fresh PWE was added to 50 mL silver nitrate (1 M) with constant stirring (150 rpm) for 20 min at 50 °C and pH 6.8. the reaction continued until a brown-colored solution was obtained due to the reduction of AgNPs. The nanoparticles were stored until further analysis and characterization.

2.3. Characterization of PPAgNPs

Spectroscopic analysis was used to describe PPAgNPs physiochemical properties. The UV–visible spectrometer (Shimadzu UV–visible 2900, Japan) in the 200–700 nm range was used to identify PPAgNPs. Transmission electron microscopy (TEM, JEOL, Japan) was used to investigate the powdered PPAgNPs, including high-resolution photographs, and a chosen area for the composition, size, and structure and shape of produced PPAgNPs were characterized. The surface charge of AgNPs was determined by Zeta potential (Nano Z2, Malvern, UK), and the size of AgNPs was evaluated by Zeta sizer. FTIR spectroscopy (Bruker, Germany) at 3,500 – 500 cm^{-1} was used to identify the active components in AgNPs; the characterization methods were followed by Saad et al., (2021a).

2.4. Phenolic content of PPAgNPs compared to PWE

Total phenolic and total flavaniods content

TPs and TFs in PWE and PPAgaNPs were measured by a Bioteck microplate reader (BioTek Elx808, Winooski, VT, USA) at 750 and 430 nm wavelengths, respectively (Herald et al., 2012; Attard, 2013). TPs were estimated with the Folin method, as follows, 100 μL of PWE or

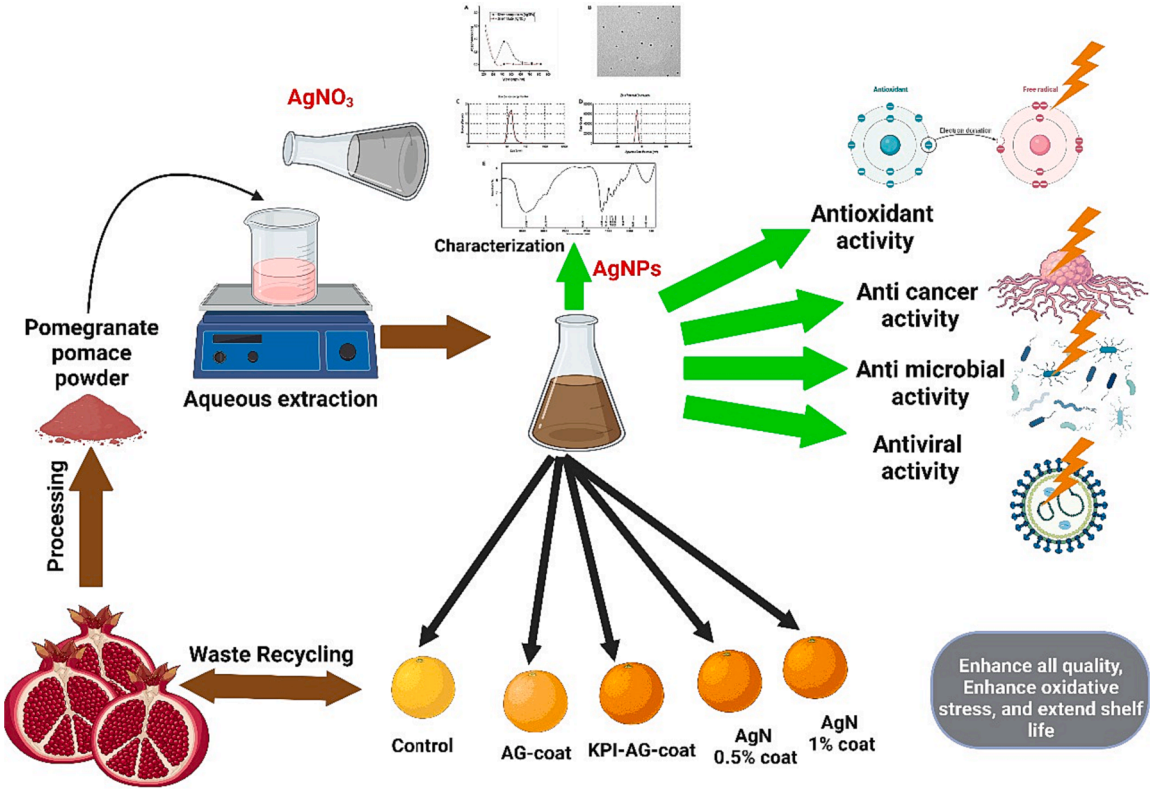

Scheme 1. Expermental layout of biological synthesis of AgNPs and its applications.

PPAgaNPs concentration was added to the respected well, then 50 μL of sodium carbonate (7.5 %) and 50 μL of diluted Folin reagent were added to each well and incubated for 30 min at 55 °C. The deep blue color was measured at 750 nm, and the total phenolic compounds' content was expressed as mg equivalent gallic acid (GAE) per gram of extract using the gallic acid standard curve.

The TFs were evaluated by the $AlCl_3$ method as follows, 100 μL of fruit juice was added to the respected well, then 50 μL ethanolic $AlCl_3$ and kept in the dark for thirty minutes. The developed yellow color was measured at 430 nm, and TFs were expressed as mg quercetin equivalent per extract using a standard quercetin curve.

HPLC-MS phenolic profile of PPAgNPs compared to PWE

Ten milliliters of the PWE or PPAgNPs solutions were filtered through a 0.2-μm filter. The filtrate, about 1–3 mL in volume, was collected for HPLC analysis. A Shimadzu LC-10AS high-performance liquid chromatography (HPLC, Japan) system with a quaternary pump, solvent degasser, an autosampler, and a C18, Gemini, 4.60 mm x 5 m, 35 °C column was used to detect phenolic chemicals. The mobile phase consisted of a gradient solvent system of water and acetonitrile with 5–60 % in formic acid with a flow rate of 1 mL/ min. The samples were automatically injected using a SIL-40Cxs autosampler. A triple-quadruple spectrometer connected to ESI detected the compounds. The MS was operated in the negative ion mode, and 35 % of the collision energy was used to induce fragmentation of the precursor ions in the MS/MS stage. The ions were identified by their mass-to-charge ratio (m/z) utilizing a full-scan mass spectrometry method that scans the entire mass range from 100 to 1500 m/z (Saad et al., 2021b).

2.5. Biological activities of PPAgNPs compared to PWE

Antioxidant

The scavenging ability of PWE and PPAgNPs was evaluated following (Jia et al., 2012). After 30 min of dark incubation, the mixture containing 0.1 mL of PWE (320 μg/mL), DR-AgNPs concentrations (20, 40, 80, 160, and 320 μg/mL), and 3 mL of DPPH solution was read at 517 nm to determine the generated colour. The following formula was used to determine the antioxidant activity of PWE and DR-AgNPs against DPPH.

$$\%\ \text{Scavenging activity} = \frac{AC - AS}{AC} \text{x } 100 \quad (1)$$

AC, absorbance control, AS, absorbance sample.

Antimicrobial

The disc assay evaluated the antibacterial and antifungal activity of PPAgNPs (Ashour et al., 2020). The pathogenic bacteria, *Listeria monocytogenes* (L.M), *Staphylococcus aureus* (S.A), *Campylobacter jejuni* (C.J), *Salmonella typhi* (S.T), and *Candida, C. glabrata* (C.G), *C. rugosa* (C.R), and *C. stellata* (C.S) were cultured overnight in a Muller Hinton (MHB) using a shaking incubator (250 rpm, 37 °C) until 1.5 x 10^8 CFU/mL. In comparison to PWE, the cultivated microorganisms were subjected to various PPAgNPs concentrations. On the surface of Petri plates, a 100 μL inoculum of bacteria and Candida was dispersed. On the plate, six-millimeter paper discs were coated with PPAgNPs or PWE in varying concentrations. The plates were incubated for 24 h at 37 °C. A ruler was used to measure the inhibition zones' sizes in mm. Levofloxacin and clotrimazole served as the positive controls to compare the antimicrobial outcomes.

Antiviral

The SARS-CoV-2 Spike protein and the ACE2 receptor produced by human cells were prevented from interacting by the SARS-CoV-2 inhibitor screening assay kit (Adipogen, California, United States). Each

microtiter plate well received a 100-μL volume of Spike RBD, which was then maintained overnight in a refrigerator. A volume of 100 μL of PPAgNPs was added to each well of a microtiter plate containing Spike RBD in order to assess the antiviral activity of PPAgNPs. The inhibitor Mix Solution was incubated for 120 min at 37 °C on the microplates that were coated with HRP-streptavidin. The reaction was stopped after 5 min by adding 100 μL of tetramethylbenzidine, and the generated color's absorbance was measured at 450 nm.

Anticancer

A neutral red assay determined the cytotoxicity of PPAgNPs compared to PWE (Repetto et al., 2008). Breast cancer cell lines (MCF-7) and human colon cancer cell lines (HCT-116) were was procured from the American Type Culture Collection (ATCC), they kept alive in full Dulbecco's modified eagle media with streptomycin and penicillin (100 mg/mL) and foetal bovine serum (10 %) at 37 °C in a humid atmosphere of 5 % CO_2. In an aseptic environment, cells were cultured in a 25 mL cell culture flask with the full media. 80 % confluence monolayer in a culture was trypsinized with 1 mL of trypsin-EDTA solution and left incubating for 2 min. After adding 5 mL of full culture medium and lightly tapping the flask to separate the cells, the reactions were stopped. The cell suspension was then transferred to a sterile falcon and centrifuged at 1800 rpm for 5 min. In one millilitre of complete medium, the pellets were redissolved. Trypan blue was used to determine the vitality of the cells after a hemocytometer had counted the cell suspension (100 % viability). The cell suspension was transferred to a sterile tube after being diluted with complete medium to a concentration of roughly 100,000 cells/ml. 200 L of a cell suspension containing around 20,000 cells was injected into the wells of the plates. For one day, the plate was maintained. Utilizing a microplate reader (BioTek, ELx808, SA, USA) to detect absorbance, cell viability was evaluated. The capacity of PPAgNPs to induce apoptosis was assessed using microplate reader fluorescence monitoring at 485/530 nm (Alsubhi et al., 2022).

2.6. In vivo safety experiment

Forty albino rats (120–150 g) were divided into four groups of ten animals. The rats received diets for a month as follows: the control group (T1) received a basal diet, the T2 group received the basal diet supplemented with 1.2 mg/kg of PWE, the groups T3, T4, and T5 received the basal diet fortified with PPAgNPs at 0.4, 0.8, and 1.2 mg/kg. At the end of the experiment, the rats were euthanized, and liver and kidney specimens were collected surgically. Blood samples were taken from the vein behind the eye (*retro*-orbital vein) to measure the levels of different chemicals in the blood (biochemical parameters).

Biochemical tests

All following determinations were done in serum: James (2001) estimatied TG, low-density lipoproteins (LDL, CH 12 31), high-density lipoproteins (HDL, CH 12 30), aspartate aminotransferase (AST), alanine aminotransferase (ALT), and malondialdehyde (MDA, MD 25 29), a marker of oxidative stress and renal function, was calculated using the thiobarbituric acid (TBA) assay. Urea (CAT no. UR 21 10) and creatinine (CAT no. CR 12 50), two other markers of renal function, were also measured. All blood biochemical parameters are determined through commercial diagnosing kits (Biodiagnostic Company, Egypt). Immunoglobulin isotypes) IgA and IgG) were assayed in ELISA (Gao et al., 2023).

Histological tests

The liver and kidney tissue samples were removed, fixed in a 15 % buffered neutral formalin solution for 48 h, dried in 70 to 100 percent ethanol, cleaned in xylene, and then embedded in paraffin. Five millimetres of paraffin were cut into slices using a microtome (Leica RM 2155, England). Hematoxylin and eosin (H&E) stain was commonly used to make histopathology sections (Suvarna et al., 2018). An optical microscope and a digital camera were used to take all sectional pictures.

Determination of inflammation factors IL-6, TNF-α

Serum samples were analyzed using an enzyme-linked immunosorbent assay for TNF-α (ng/mL) and IL-6 (pg/mL) cytokine levels. The Human IL-6 Bioassay Technology Laboratory (BT-Lab) ELISA kit and Human TNF-αELISA kit were used. Each well received 40 mL of serum before receiving 50 mL of streptavidin-HRP for the sample and control wells. After an hour of incubation at 37 °C under cover, the plate was washed five times with wash buffer. Each well received 50 L of substrate solution at first, then 50 L of substrate solution B. After that, the sample was incubated for 10 min in the dark at 37 °C. A microplate reader was used to read the OD at 450 nm after adding the stop solution (50 L) to the wells for 10 min to stop the reaction.

2.7. Preparation of functional AgNPs coating

5 gm of white kidney peptide (KPI) were homogenized in 100 mL and stirred for thirty minutes at 80 ℃; Arabic gum (0.5, 1, and 1.5 % w/w) also dissolved in distilled water at 50 ℃ for 60 min. The KPI and AG solution was mixed with glycerol (30 % w/w), stirred for an hour at 60 ℃, and adjusted to 9. The optimum concentration of AG to prepare film was 0.5 %. The prepared AgNPs at two concentrations, 1 and 2 %, were slowly added into the already prepared KPI/0.5 % AG film and sonicated for 20 min, then the KPI/AG/AgNPs were kept for the coating experiment (Saad et al., 2021c).

2.8. Coating experiment of "Vermont" mandarin fruit

The fruits were sanitized for 2 min with NaClO (0.04 %), then air dried at 25 °C and RH 65 %. With the uncoated fruit serving as the control, four fruit groups were created. The remaining three fruit groups were immersed for three minutes in KPI, KPI/AG, and KPI/AG/AgNPs solutions and then dried at room temperature. Each of the four sets of fruits was kept at 25 °C and 65 % relative humidity.

2.9. Physiochemical properties of fruits

Fruit pH

Ten mL of fruit juice was homogenized, and the residues were discarded. The pH meter was used to measure the fruit pH.

Titratable acidity (TTA)

Using standard procedure 942.15, the TTA in fruit juice was calculated as a percentage of citric acid AOAC (2012). The citric acid in 10 mL of fruit juice was estimated using sodium carbonate (0.1 N) a phth as an indicator.

Total soluble solids (TSS)

Using a C10 Abbe refractometer, the total soluble solids (TSS) of the fruit juice were calculated (VEE GEE, Thermofisher Scientific, USA). On the glass in front of the refractometer, a few drops of the fruit juice were applied, and the results were noted.

2.9.1. Antioxidant activity

The scavenging ability of mandarin fruit juice was evaluated as sec 2.5.

2.9.2. Antioxidant enzymes

Catalase Activity

Catalase activity was measured by He et al. (2020). One gram of rind was ground in a blender with 10 mL of phosphate buffer at a pH of 7, EDTA, and urea. The mixture was blended for 10 min, then spun in a centrifuge at 10,000 revolutions per minute for 15 min while kept cool. The obtained supernatant (0.1 mL), 0.5 mL of H_2O_2, and 2.5 mL of phosphate buffer (pH 5) was added to a cuvette., and the OD at 240 nm was measured trice (one minute each) using a spectrophotometer. One enzymatic unit is equal to a 0.01 per minute increment in absorbance. The obtained values were converted to U/mL/DW using the given equation:

$$Catalaseactivity = \frac{Af - As \times reactionvol}{timeinterval \times enzymevol}$$

Where: Af = final absorbance; As = initial OD; reaction vol. = 3; time interval = 3; enzyme vol = 0.1 mL.

The peroxidase enzyme's action (POD)

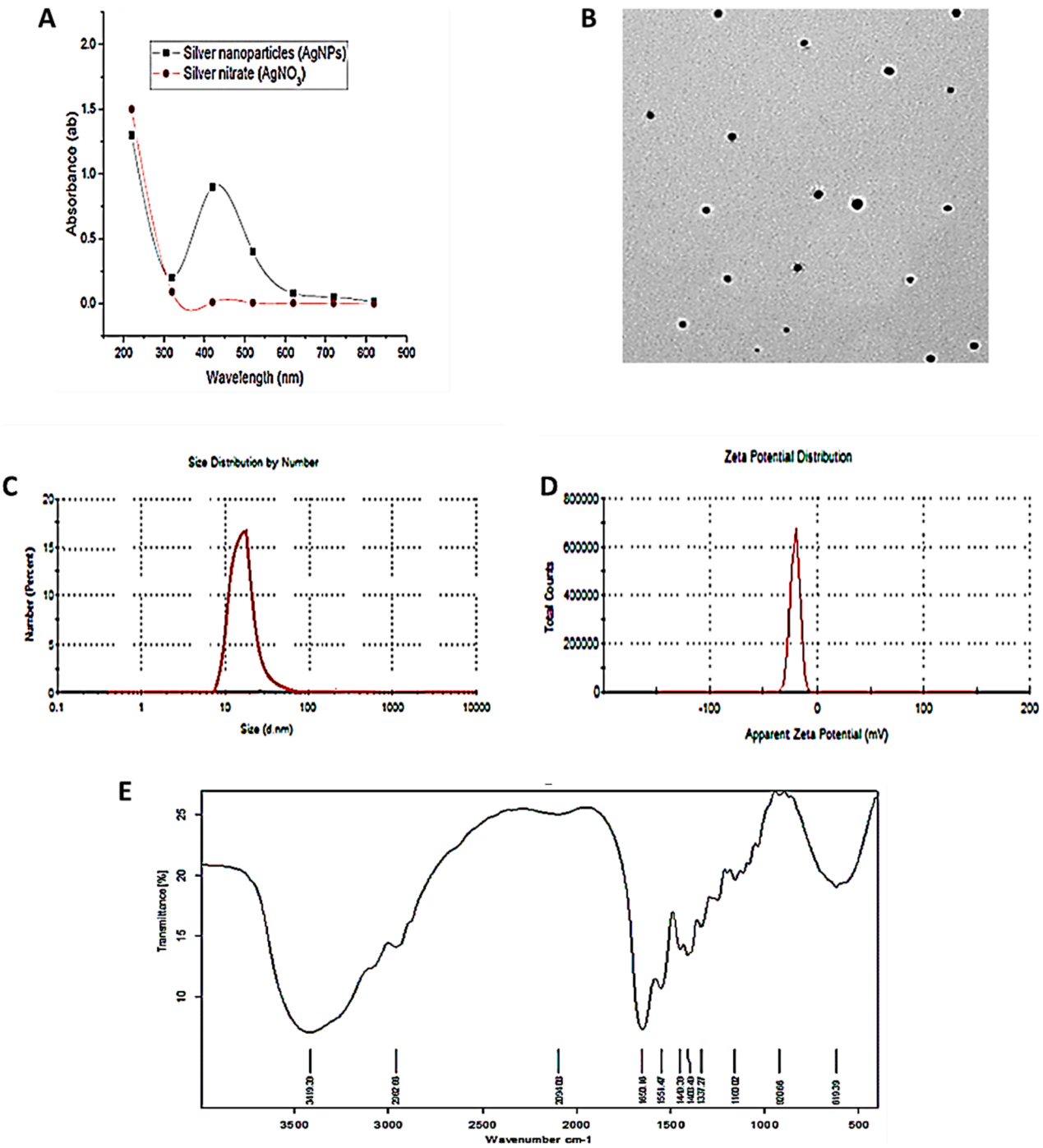

Fig. 1. Characterizing PPAgNPs synthesized by pomegranate waste extract (A) UV absorbance at 430 nm, (B) TEM image with a size of 15–55 nm, (C) zeta sizer calculates the size of nanoparticles 20 nm, (D) zeta potential calculates the charge on nanoparticles of −25.98 mV, (E) FTIR for detection of active groups responsible for PPAgNPs reduction.

POD's activity was assessed by Hussein et al. (2019) at OD 470 nm. The fresh rind was mixed for ten minutes in phosphate buffer containing EDTA and PVPP; the mixture was centrifuged, and the enzymatic supernatant (100 μL) was added to 2.5 mL guaiacol (3 %) in phosphate buffer and incubated for thirty minutes then 500 μL of H_2O_2, and the OD of developed color was read at 470 nm. The peroxidase content (U/mL/DW) was calculated in the equation:

$$Peroxidaseactivity = \frac{Af - As \times reactionvol}{timeinterval \times enzymevol}$$

Activity of Superoxide Dismutase (SOD)

The SOD activity was assessed by He et al., (2020) at 560 nm. 0.1 mL of enzymatic supernatant was added to 1 mL Phosphate buffer (pH 5), 1 mL distilled water, 0.3 mL methionine (22 μM), and 0.1 mL nitroblue tetrazolium (20 μM). The vial was then exposed to ultraviolet light for 15 min before adding 100 L of 0.6 M riboflavin was added (as a substrate). One unit of Superoxide dismutase refers to the quantity of enzyme necessary to prevent the decrease of NBT by 50 percent; the OD at 470 nm was measured in trices (one minute each) using a spectrophotometer. SOD activity (U/mL/DW) of rind was calculated in the equation.

$$SODactivity = \frac{Af - As \times reactionvol}{timeinterval \times enzymevol}$$

2.10. Statistical evaluation

The variation between the data means for the triplicate values was examined using one-way ANOVA at p 0.05. The LSD was used to contrast differences in average results. The statistical analysis was completed using SPSS 23.0 software.

3. Results

3.1. Characterization of PPAgNPs

When PWE extract is added to a solution of silver nitrate, the color changes from no color to brown, suggesting the fabrication of PPAgNPs. Fig. 1A demonstrates that the resulting PPAgNPs absorb UV at 430 nm, verifying the Ag transformation. The TEM image (Fig. 1B) of the produced PPAgNPs revealed spherical particles ranging from 15 to 55 nm. The zeta sizer image in Fig. 1C shows the exact size of PPAgNPs is 20 nm. At the same time, the net surface charge was negative of −25.98 mV detected by zeta potential (Fig. 1D); Eight bands were seen in the FTIR spectra of PWE, whereas eleven bands between 3500 and 500 cm^{-1} were visible in the spectrum of PPAgNPs (Fig. 1E). These bands imply that the structure of PPAgNPs contains active groups like phenolic and alcoholic OH, NH, and NH_2. The OH and NH_2 groups have a frequency of 3,419.39 cm^{-1}, while the CH group has a frequency of 2,982.66 cm^{-1}. Alkyne group is related to the band at 2094 cm^{-1}, while alkanes, alkenes, and aromatic compounds are related to the bands at 1,650.09 cm^{-1} and 1,373 cm^{-1}, respectively. Esters were present, as indicated by bands at 1150 cm^{-1}, while halide compounds were indicated by bands at 617.39 cm^{-1}.

3.2. Polyphenol components in PPAgNPs

3.2.1. Total phenolic and flavonoid compounds

Fig. 2 show the phenolic compounds in PWE and PPAgNPs were (310 and 520 mg/g). The flavonoid content was 180 and 250 mg/g, respectively, with a relative increase of 48 % over the reduction agent PWE.

3.2.2. Phenolic compounds profile

As described above, the detected compounds in the phenolic profile

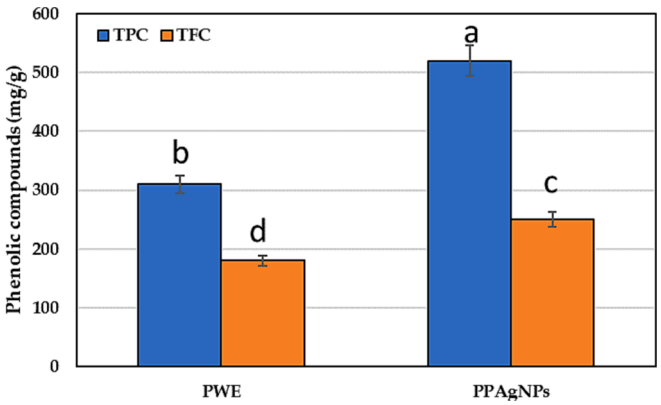

Fig. 2. The phenolic and flavonoid compounds were assessed as gallic acid and quercetin equivalent for PWE and PPAgNPs.

are increased in nanoparticles than in the extract. Compounds in PPAgNPs and PPWE were described by mass spectrometry employing both positive and negative ion modes, while most compounds were discovered using the negative mode (Table 1). The LC/MS spectra detected 19 phenolic compounds; Punicalagin derivatives were the main compounds in LC/MS profile, accounting for 83 %, flavonoids 3.6 %, Ellagic acid derivatives 8.5 %, and anthocyanins 5 %.

Granatin B is the primary phenolic acid (66.2 mg/100 g). It was detected at deprotonated molecular ions at 950 *m/z* and fragment ions at 301 *m/z*. This fragmentation pattern has been documented in the library for Castalagin derivative and Granatin B. Consequently, Q-TOF was used to determine the exact mass, comparing the fragmentation pattern with the METLIN database. So, Granatin B was detected compound at RT 9.3, followed by Bis-HHDP hexoside, which was detected at deprotonated ion at 780 *m/z* and FI at 301 *m/z*. Concerning ellagic acid derivatives,

Table 1
Phenolic compounds content in PPAgNPs and PWE detected by LC/MS.

No	Detected compounds	g/100 g		[M−H]- *m/z*	FI *m/z*
		PPWE	PpAgNPs		
1	Gallic acid	11.6 ± 0.2	19.2 ± 0.5	168.9	126
2	Ellagic acid	10.5 ± 0.3	15.1 ± 0.4	301	230
3	Ellagic acid pentoside	2.5 ± 0.0	4.1 ± 0.5	477	301
4	Ellagic acid deoxyhexoside	2.9 ± 0.5	4.6 ± 0.1	450	301
5	Ellagic acid hexoside	3.2 ± 0.6	4.7 ± 0.6	461	301,271
6	Hyterophyllin A	29.66 ± 0.9	45.2 ± 0.9	802	650
7	Procyanidin	3.6 ± 0.1	5.9 ± 0.1	570	441
8	Cyandin pentoside	2.01 ± 0.2	3.6 ± 0.8	417	288
9	HHDP-hexoside	26.5 ± 0.3	33.1 ± 0.9	480	301
10	Bis-HHDP hexoside	49.2 ± 0.9	56.8 ± 0.4	780	301
11	Galloyl hexoside	32.6 ± 0.1	36.2 ± 0.5	330	271
12	Castalagin derivative	21.9 ± 0.2	24.5 ± 0.8	960	301
13	Feruloyl coniferin	3.6 ± 0.1	6.2 ± 0.2	516.9	271
14	Coumaroyl hexose	0.89 ± 0.8	2.0 ± 0.0	320.8	163
15	Caffeoylquinic acid	1.5 ± 0.2	3.3 ± 0.1	355	191
16	Pelargonidin	1.2 ± 0.1	2.7 ± 0.3	270	180
17	Delphinidin	2.8 ± 0.0	4.6 ± 0.2	626	302
18	Phlorizin	0.9 ± 0.2	2.1 ± 0.5	434.9	165
19	Granatin B	61.2 ± 0.1	66.2 ± 0.4	950	301

Fragmentation ion (FI) $n = 3$, values are presented mean of triplicate data ± SD, $p \leq 0.05$ indicate significant differences.

ellagic acid was the main compound (15.1 mg/100 g) detected at molecular ion 301 and confirmed at fragment ion (230 *m/z*) by Q-TOF, followed by ellagic acid deoxy hexoside at 450 *m/z*. Furthermore, procyanidin was the prominently detected anthocyanin with 6 mg/100 g, seen at molecular ion 570 *m/z*, followed by Delphindin at 626 *m/z*.

3.3. Biological activity of PPAgNPs

3.3.1. Scavenging ability

In our study, PPAgNPs have high phenolic, flavonoid, and tannin correlated with high radical scavenging. Comparable to the antioxidant activity of ascorbic acid and DRE, 94 % of DPPH free radicals were substantially neutralized by PPAgNPs (Fig. 3). 20 μg/mL of PPAgNPs considerably scavenged 50 % of DPPH free radicals.

3.3.2. Cytotoxicity against cancer cell lines

Fig. 4 shows that PPAgNPs have significant cytotoxicity against two cancerous cell lines, breast (MCF-7) and colon (HCT) cancer populations comparing PWE and anticancer medicine DOX. Cancerous cells' death increased concentration-dependent ($p = 0.016$). PPAgNPs (320 μg/mL) lowered the number of liver cancer (HCT) and breast cancer (MCF-7) cell lines by 78 and 80 percent, respectively, respectively, comparing PWE and DOX by 75 and 76 %, confirmed by the microscopic images, where the cell death excel PPAgNPs than PWE and DOX (Fig. 4A and B). This is an indicator for vindicating oxidative stress on human cells. When PPAgNPs (320 g/mL) were applied to the cancer cell lines of the breast (MCF-7) and colon (HCT), more caspase-3 activity was observed in Fig. 4C, which corresponds to an increase in the death of cancer cells.

3.3.3. Antimicrobial

The investigated microorganisms were significantly resistant to PPAgNPs' antibacterial effects (Table 2). The concentration-dependent IZDs ranged from 11 to 36 mm against tested bacteria and 12–33 mm against tested *Candida*, who excelled in bacterial or the zones of clotrimazole. The microorganisms most vulnerable to PPAgNPs at 320 g/mL (36 mm) were SA and CJ (27 mm). *Candida gelberta* was the most resistant to the reported inhibitory zone (24 mm) of PPAgNPs, followed by CR (28 mm) compared to PWE and antibiotics The lowest PPAgNPs concentration against the tested microorganisms, which ranges from 15 to 20 g/mL, is shown in Table 2. In comparison to PPWE and antibiotics, S. aureus had the lowest MIC (15 g/mL), CJ had the highest (20 g/mL), while MBC and MFC ranged from 15 to 40 g/mL (Fig. 5).

3.3.4. Antiviral activity

Fig. 6 shows that PPAgNPs have potent antiviral activity against COVID. The inhibition in the virus correlated with PPAgNPs concentrations. PPAgNPs (320 μg/mL) successfully inhibited COVID by 82 % compared to AC384, which inhibited the virus by 78 %. The IC50 of PPAgNPs was 80 μg/mL.

3.4. Safety experiment

3.4.1. Serum biochemical tests

Table 3 demonstrates that all biochemical indicators evaluated in PWE rats significantly increased ($p = 0.039$) compared to the other groups but still at normal levels. However, the liver and kidney markers in the serum of rats administered PPAgNPs for four weeks decreased considerably ($p = 0.031$) (Table 3). PWE rats had lower levels of TP and GSH than the control group (Table 3). The diet system of PPAgNPs (160 μg/g) significantly ($p = 0.032$) reduced the concentrations of the kidney parameters. Concerning MDA, it can have been found that the PPWE group was 49.5 μmol/L, which is considered higher than the control (45.6 nmol/ml) but in the normal ranges. There is a slight decrease in rats fed PPAgNPs (1 6 0) with 48.6 nmol/ml. In addition, PWE showed a slight increase in kidney markers compared to PPAgNPs and control ($p = 0.041$; Table 3). Because PPAgNPs include more antioxidant chemicals than the PWE group, the PPAgNPs rats had lower urea and creatinine levels than the PWE group; PPAgNPs rats (160 g/g) also shown a drop ($p = 0.29$) in renal indicators when compared to PWE rats. The kidney markers reduced by natural complexes by converting into uric acid in the urine with the assistance of blood flow in the kideny. Table 3 demonstrates that adding PPAgNPs to the diet at three doses (80, 160, and 320 μg/g) retained TG, LDL, and cholesterol levels at the control level while boosting HDL levels dose-dependently. The rats' diet supplemented with PPAgNPs (80 μg/g) had the lowest TC level (64.2 mg/dl) compared to PPWE and control. Table 3 results ensure that PPWE and PPAgNPs are safe and can be used as a medicine.

3.4.2. Histological study

The examined (Liver and kidney) sections in group (1) (Control) showed standard histological structure in all organs (Fig. 7A). The examined liver sections in Group 2 (PPAgNPs 80) revealed normal hepatic parenchyma with normal central veins and hepatic cords. The kidney showed normal renal parenchyma (Fig. 7B). Tissue sections in Group (3) 160 μg/kg showed normal organ histological structure during the study period.

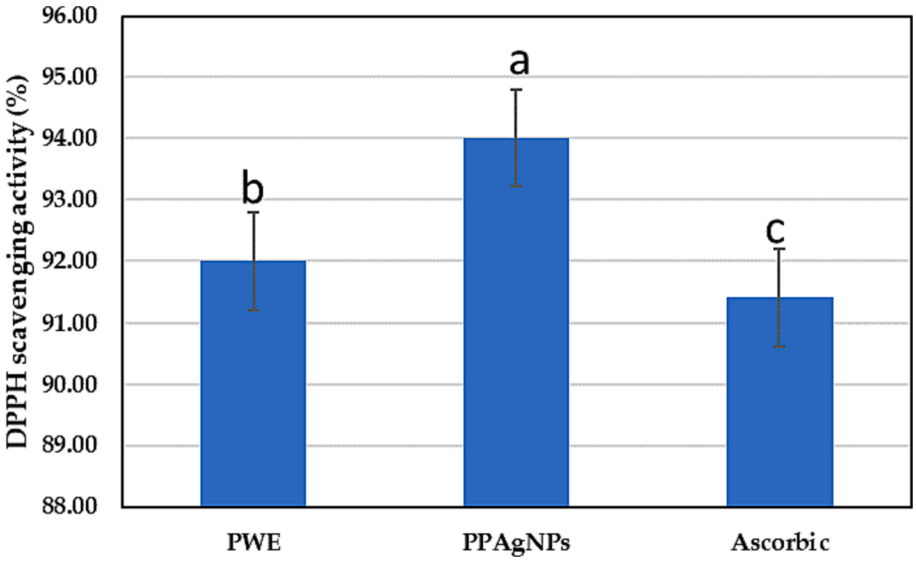

Fig. 3. Antioxidant activity of PPAgNPs and PWE compared to ascorbic acid.

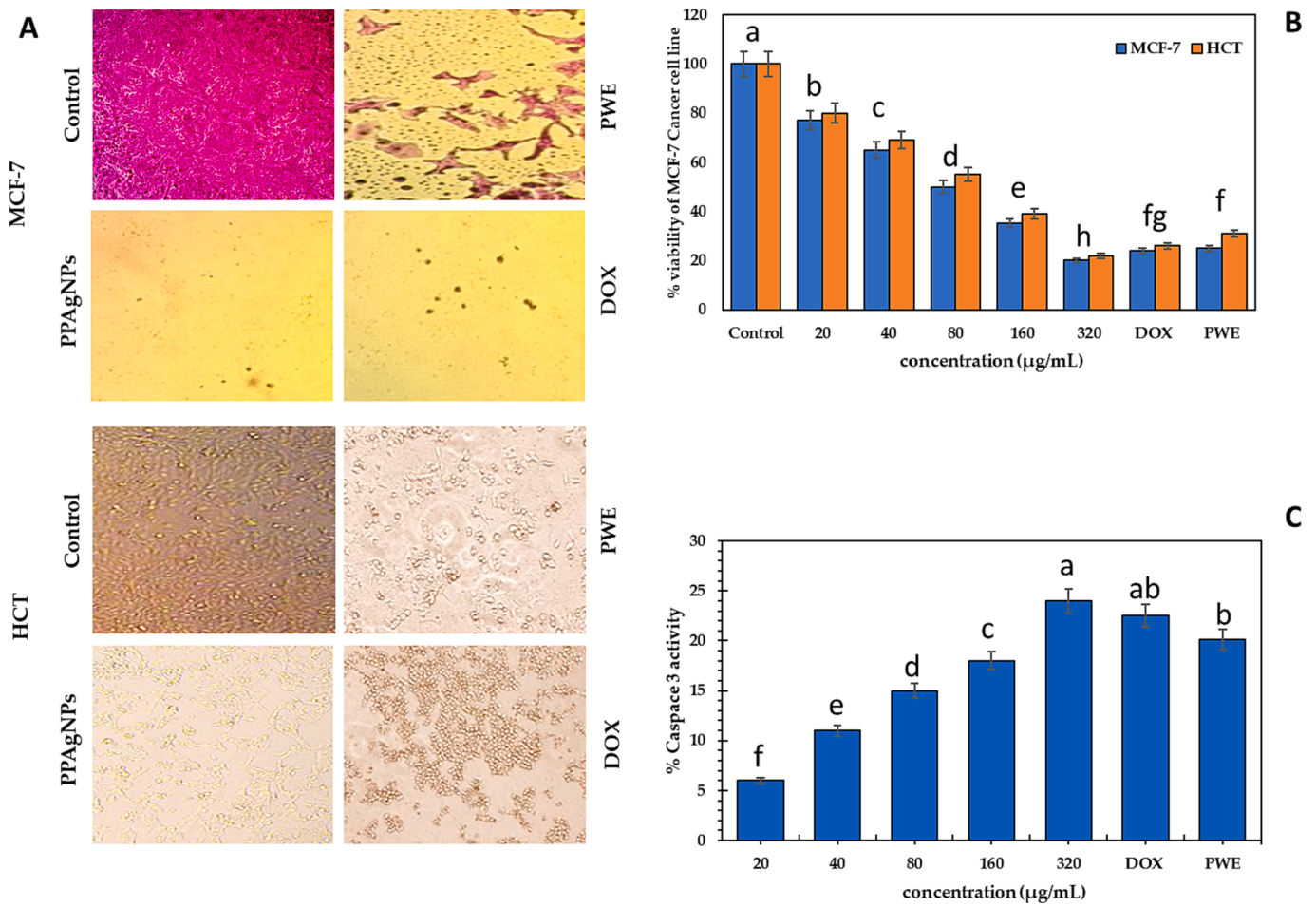

Fig. 4. (A) The effect of PPAgNPs on the viability of MCF-7 and HCT cancer cell lines. (B) % MCF-7 HCT cancerous cell lines vitality affected by PPAgNPs, PWE and DOX, (C) Caspase-3 activity.

Table 2
Inhibition zones, MIC, and MBC of PPAgNPs against tested microorganisms compared to PWE and antibiotics.

Pathogenic Bacteria	PPAgNPs (µg/mL)/IZDs (mm)					PWE	Antibiotic	MIC	MBC
	20	40	80	160	320	320	320		
LM	11 ± 0.2c	14 ± 0.2c	19 ± 0.3d	22 ± 0.2d	29 ± 0.2c	27 ± 0.3c	33 ± 0.1b	15 ± 0.2	25 ± 0.2
S. A	15 ± 0.1a	19 ± 0.1ab	25 ± 0.5a	29 ± 0.3a	34 ± 0.1a	32 ± 0.1a	36 ± 0.1a	10 ± 0.2	15 ± 0.1
CJ	–	11 ± 0.5d	15 ± 0.4e	22 ± 0.6d	27 ± 0.2d	25 ± 0.4d	29 ± 0.2e	20 ± 0.1	40 ± 0.6
S. T	–	14 ± 0.2c	18 ± 0.5d	23 ± 0.4c	29 ± 0.1c	26 ± 0.0c	30 ± 0.0c	20 ± 0.3	35 ± 0.5
Pathogenic Fungi								MIC	MFC
CG	–	16 ± 0.1b	18 ± 0.1e	20 ± 0.1e	24 ± 0.0e	22 ± 0.9e	27 ± 0.2d	20 ± 0.6	35 ± 0.5
CR	12 ± 0.5c	19 ± 0.5ab	21 ± 0.5c	24 ± 0.8c	28 ± 0.3d	26 ± 0.1c	30 ± 0.1c	15 ± 0.4	30 ± 0.2
CS	14 ± 0.9b	20 ± 0.1a	23 ± 0.8b	26 ± 0.7b	31 ± 0.1b	29 ± 0.5b	33 ± 0.3b	10 ± 0.8	15 ± 0.3

$n = 3$, data are presented as the mean of triplicate data ± SD, levofloxacin, bacterial antibiotic, and clotrimazole as a fungal antibiotic. *Listeria monocytogenes* (LM); *Staphylococus aureus* (S.A); *Campylobacter jejuni* (CJ); *Salmonella typhi* (ST); *Candida glabrata* (C.G); *Candida rugosa* (C.R); *Candida stellata* (C.S). a-e lowercase letters indicate significant differences.

Also, the hepatic sections in Group (4) 320 µg/kg showed normal hepatic lobules and inflammatory portal infiltrations. Other groups revealed normal peribiliary lymphocytic infiltrations adjacent and acute cell swelling hepatic cells.

3.4.3. Determination of inflammation factors IL-6, TNF-α

TNF-α and IL-6 are major proinflammatory cytokines that indicate early stages of inflammation. Fig. 8 shows that PPAgNPs treatments downregulated the level of TNF-α and IL-6 compared to control and PWE, where PPAgNPs 320 showed lower levels of TNF-α and IL-6 29.8 ng/ml and 17.2 pg/mL, respectively, indicating the protective effect of green sliver nanoparticles in mitigating the early cell inflammation.

3.5. Coating experiment of postharvest Vermont mandarin

3.5.1. Chemical properties

Table 4 shows that TSS significantly increased with the storage period; TSS accumulation is the most critical maturation and ripening marker of fruit quality; the initial TSS in control fruit was 11.5 %, which increased to 14.7 % at 60 d; also, KPI/AG/AgNPs 1 % coated fruit showed the same trend where the TSS increased from 13 % on day 15 into 14.9 % on day 60. On the other hand, the acidity of coated fruit

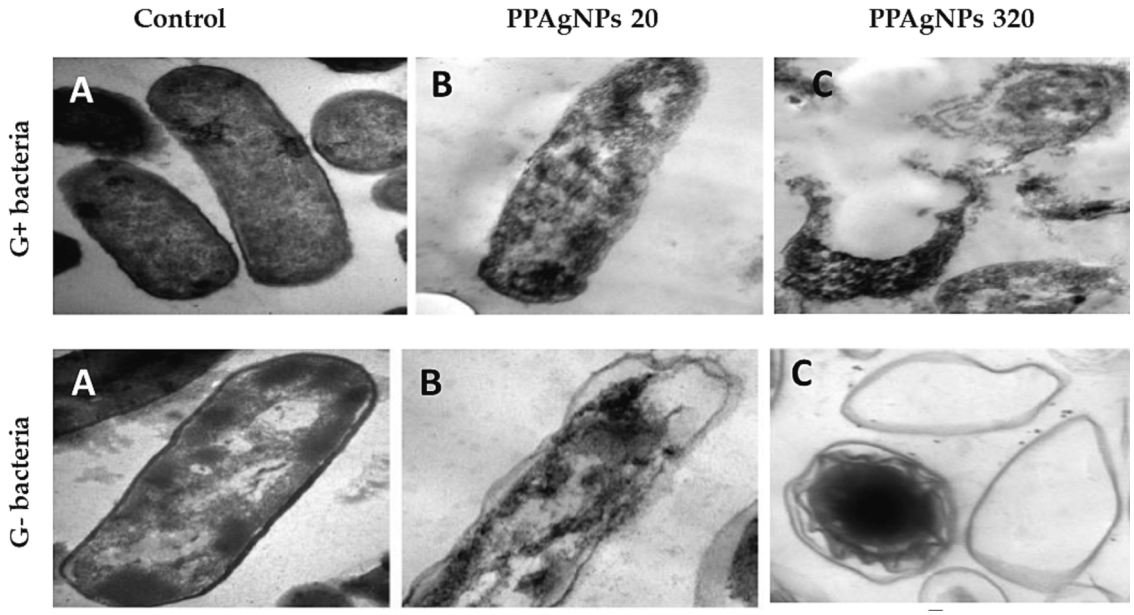

Fig. 5. TEM image about the antimicrobial mechanism of PPAgNPs against pathogenic bacteria (A) control, (B) PPAgNPs interact with membrane of bacteria, (C) PPAgNPs enter incide cell and react with cell componants.

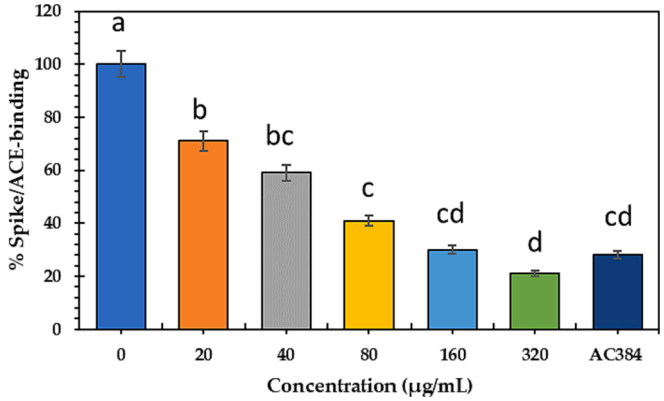

Fig. 6. Antiviral activity of PPAgNPs against COVID compared to AC384.

decreased with storage time, where the TA of KPI/AG/AgNPs 1 % covered fruit reduced by 39 %; however, uncoated fruits showed an increase in TA, probably owing to a quick concentration impact of organic acids caused by a more significant loss of fruit moisture. In contrast, the gradual decrease in coated fruits' TA because the Coating reduced the respiration rate.

3.5.2. *Antioxidant content and antioxidant activity of fruit*

Table 5 demonstrates how different coatings and storage times significantly (p0.05) impact the antioxidant content and activity of mandarin fruits. The antioxidant activity of KPI/AG/AgNPs 1 % coated fruits is attributable to phenolic and flavonoid contents, where scavenged 90 % of DPPH free radicals compared to 75 % in control, after 60 days of storage, the % AA decreased to 49 and 75 % in uncoated and KPI/AG/AgNPs 1 % coated fruits, respectively.

3.5.3. *Antioxidant enzymes*

SOD activity declined as the storage period increased, which recorded the highest values after 60 d in KPI/AG/AgNPs 1 % coated fruits (15 U/mL/min) with a relative increase of 53 % over uncoated fruit (Fig. 9A). In Fig. 9B, the peroxidase activity increased during the storage period (30 days) and then gradually decreased. The highest activity was observed at 30 d, which reached 30 U/mL/min in KPI/AG/AgNPs 1 % coated fruits with a relative increase of 50 % over the control, indicating the enhancing effect of peptide and silver nanoparticles in the Coating.

Catalase activity was reduced with the storage period in Fig. 9C. The KPI/AG/AgNPs 1 % coated fruits have the highest catalase activity (17.5 U/mL/min) compared to 10 17.5 U/mL/min for the control sample; the CAT activity increased with coating treatments from KPI to KPI/AG/

Table 3
The effect of diet supplemented with PPAgNPs on blood biomarkers of Albino rats.

Serum parameters / Liver parameters	Control	PWE	PPAgNPs (µg/g)		
		320 µg/g	80	160	320
ALT	45.3 ± 0.1^{c}	51.2 ± 0.3^{a}	45.9 ± 0.1^{b}	48.5 ± 0.3^{b}	59.1 ± 0.2^{b}
AST	33.6 ± 0.3^{c}	43.5 ± 0.2^{a}	35.2 ± 0.2^{b}	37.3 ± 0.2b^{c}	41.9 ± 0.3^{bc}
Kidney parameters					
Urea	17.6 ± 0.1^{c}	21.5 ± 0.1^{a}	16.9 ± 0.3^{b}	19.9 ± 0.5^{c}	22.9 ± 0.4^{bc}
Creatinine	0.39 ± 0.06^{d}	0.45 ± 0.02^{a}	0.41 ± 0.02^{b}	0.46 ± 0.01^{c}	0.52 ± 0.1^{bc}
Oxidative stress parameters					
MDA	45.6 ± 0.2^{c}	49.5 ± 0.9^{a}	46.2 ± 0.1^{b}	48.6 ± 0.2^{b}	52.1 ± 0.0^{b}
GSH	56.9 ± 0.5^{a}	57.8 ± 0.0^{c}	55.3 ± 0.2^{b}	58.6 ± 0.3^{a}	59.8 ± 0.2^{a}
TP	6.9 ± 0.8^{a}	6.1 ± 0.3^{b}	6.3 ± 0.3^{b}	6.6 ± 0.5^{a}	7.2 ± 0.1^{ab}
Lipid profile					
LDL	17.3 ± 0.0^{c}	20.2 ± 0.1^{a}	24.9 ± 0.2^{b}	23.5 ± 0.3^{b}	24.0 ± 0.2^{bc}
HDL	37.7 ± 0.3^{ab}	41.5 ± 0.2^{c}	38.9 ± 0.3^{a}	42.3 ± 0.3^{b}	44.5 ± 0.2^{a}
TG	78.9 ± 0.2^{c}	82.6 ± 0.3^{a}	80.9 ± 0.2^{b}	82.9 ± 0.1^{c}	85.9 ± 0.3^{bc}
TC	65.7 ± 0.3^{c}	77.2 ± 0.7a	64.2 ± 0.1^{b}	72.3 ± 0.5^{c}	77.3 ± 0.6^{bc}

$n = 3$, The values are presented mean of triplicate data ± SD; lowercase letters in each raw indicate significant differences. malondialdhyde (MDA), and raised glutathion reduced (GSH), total protein (TP), aspartate aminotransferase (AST), alanine aminotransferase (ALT), triglycerides (TC), total cholesterol (TC).

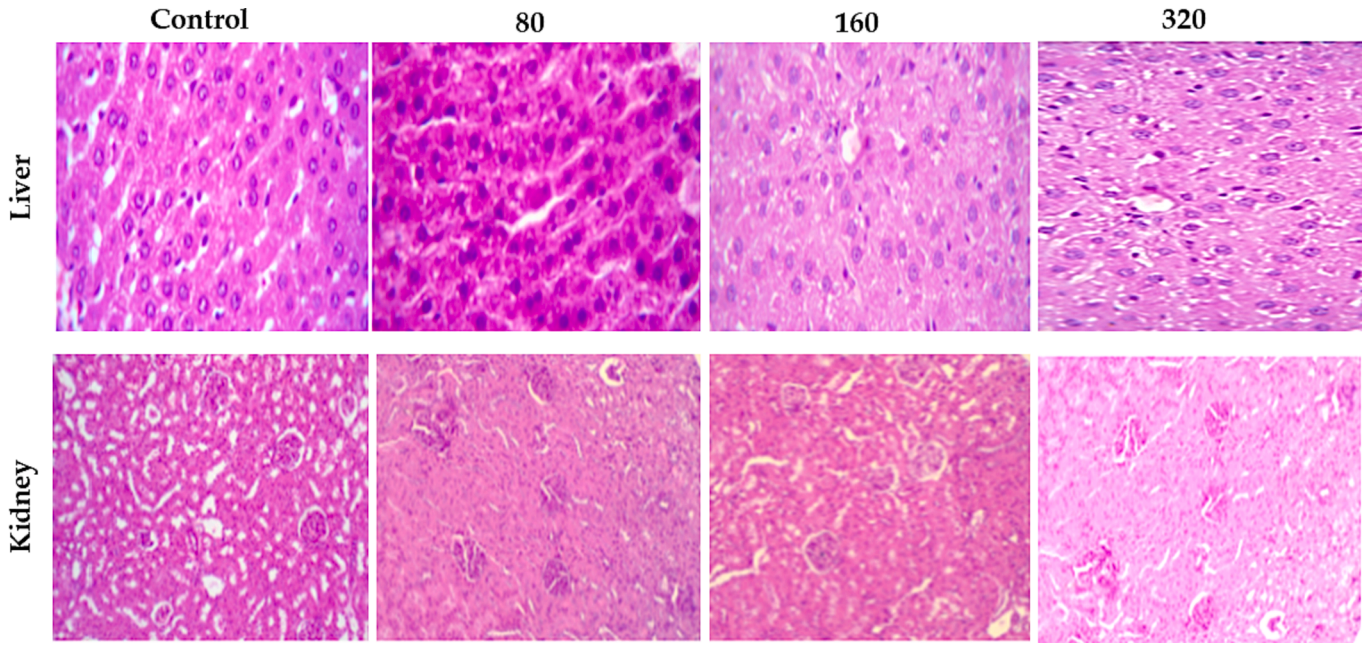

Fig. 7. Histology of liver and kidney tissue of albino rats fed dietary PPAgNPs as a medicine for stress for 30 days. All images showed normal tissues of liver and kidney under the tested AgNPs with no differences about control.

AgNPs 1 %.

4. Discussion

Green nanoparticles possess distinct biological properties because of the accumulation of phenolic and flavonoids and active groups (Chung et al., 2018); the oxidation of OH in phenolic compounds generates a quinoid structure, which increases the phenolic content in nanoparticles more than the extract, boosting phenolic content and guaranteeing nanoparticle suspension stability (Esmaeilzadeh Kenari and Razavi, 2022). The variation in polyphenols in raw plant material is influenced by a number of variables, such as the environment and the growing soil (Ranjah, 2019). In parallel with our results, (Saad et al., 2021a) found that pomegranate peel-AgNPs have rich phenolic content with a relative increase of 10–75 % over the pomegranate peel extract; also, the results of phenolic profile agree with Adje et al. (2008) and Ebada et al. (2023), who found that cyanidin-3-O-rutinocide was the main compound in pomegranate waste extract.

Because of high phenolic content of AgNPs, a 5 μg/ml concentration, green silver nanoparticles produced by *M. frondosa* leaf extract have displayed 91 % scavenging activity, while our results scavenged the same percentage of free radicals at 20 μg/ml. Flavonoids and phenolic compounds are advantageous in the prevention and treatment of harmful diseases due to their antioxidant qualities. Therefore, the higher antiradical activity near the control ascorbic acid is primarily due to the active components on the surface of green produced nanoparticles (Sreelekha et al., 2021).

Caspase-3 is a key enzyme that cause apoptosis. It can activate before or during cell death (Yadav et al., 2021). In this study, the PPAgNPs inhibited breast and colon cancer cell viability, an indicator for vindicating oxidative stress on human cells. Our results exceeded the results of Shejawal et al. (2021), discovered that lycopene-enriched tomato extract-produced silver nanoparticles showed significant anticancer effect against the cancer cell lines HeLa, COLO320DM, and H29. The strength of the reducing agent is what causes the discrepancies in values..

PPAgNPs' antibacterial activity was verified by Kemala et al. (2022) the antibacterial activity of AgNPs produced by *Calotropis gigantea* against *Staphylococcus aureus*, *Escherichia coli*, and *Candida albicans*, with inhibition zones of12.05, 11.29, and 9.02 mm, respectively. Our findings demonstrated more robust antibacterial activity than (Ferreira et al., 2022), who discovered that the MIC of AgNPs produced by Raddi leaves extract ranged from 250 to 1000 μg/mL.

The TEM results are comparable very well with those found by Attallah et al. (2022), who stated that many pits and gaps were observed in bacterial cells when exposed to 50 μg/ml AgNPs and the cell membrane of *Escherichia coli* was incomplete, indicating the bacterial cells were damaged severely. They observed that the Staphylococcus aureus cell walls were broken down when exposed to 320 μg/ml AgNPs for 12 h, releasing the cellular contents and becoming collapsed. It was demonstrated in this study. According to (Gallón et al., 2019), the antibacterial activity of AgNPs was more significant in Gram-negative than G + bacteria. These phenomena can be attributed to the difference in cell wall width between G+ (30 nm) and G- (3–4 nm) bacteria, whose cell walls are primarily peptidoglycan. In addition, (Abdelsattar et al., 2021) demonstrated that AgNPs might bind and then inter inside the cell wall.

The obtained findings showed that our antimicrobial agent was more effective at killing bacteria than the antimicrobial agent used, Ferreira et al. (2022), who discovered that the MIC of synthetic AgNPsby aqueous extract of *Schinus terebinthifolius* Raddi leaves ranged between 250 and 1000 μg/mL. The antimicrobial mechanism of AgNPs depends on the fact that silver nanoparticles may cause structure and function changes in the microbial cellular membrane of bacteria or fungi, i.e., affecting the membrane permeability and potential and blocking the membrane-attached respiratory proteins, which upsets the cell's equilibrium and causes microbial cell death.

AgNPs can prevent many viral infections by suppressing virus infection in cells or directly inactivating the viruses (Morris et al., 2019). AgNPs initially bind with the viral surface, destroying the viral genomic material or preventing its penetration of the cell membrane. Additionally, AgNPs attach to the virus to prevent it from connecting with the cell membrane; the AgNPs also block the nucleocapsids of the viral organism. In addition, silver nanoparticles (AgNPs) can attach to the genetic material of viruses, preventing them from replicating in the host cell. Finally, they disrupt biological mechanisms such as protein synthesis to prevent viral multiplication. However, some metals possess antiviral properties (Ratan et al., 2021).

The high phenolic and flavonoid content in PPAgNPs and PWE

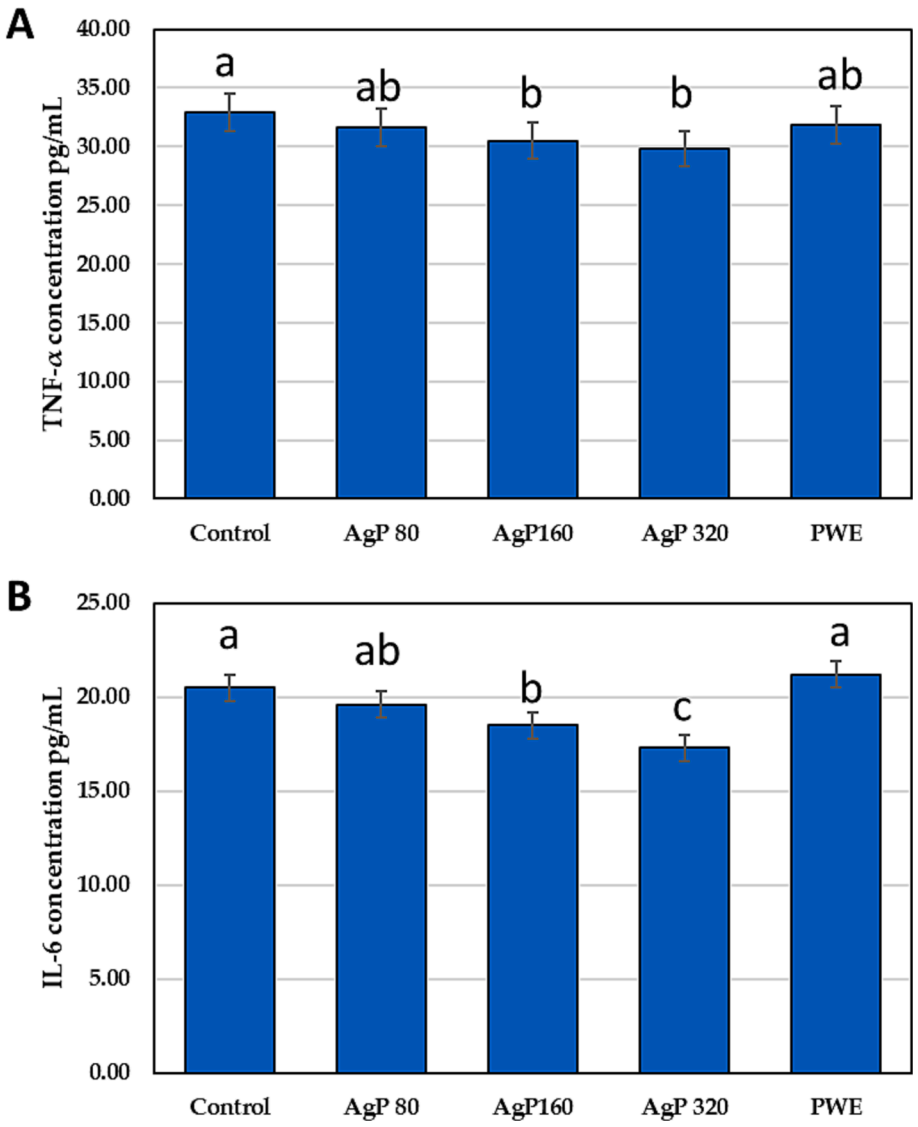

Fig. 8. Gene expression analysis of IL6 and TNF-α of albino rats fed dietary PPAgNPs as a medicine for stress for 30 days.

Table 4
Physiochemical properties (% Acidity and TSS) of fruit juice during cold storage of 15, 30, 45, and 60 days.

Treatments	TSS (%)				Mean	Acidity (%)				Mean
Storage (days)	**15d**	**30d**	**45d**	**60d**		**15d**	**30d**	**45d**	**60d**	
Control	11.5 ± 0.1	13 ± 0.2	13.8 ± 0.2	14.7 ± 0.3	**13.25^{ab}**	1.3 ± 0.1	1.5 ± 0.01	1.65 ± 0.1	1.8 ± 0.01	**1.56^{a}**
C1	11.6 ± 0.1	12.8 ± 0.6	13.5 ± 0.1	14.5 ± 0.2	**13.1^{b}**	1.5 ± 0.2	1.3 ± 0.01	1.35 ± 0.1	1.3 ± 0.02	**1.36^{c}**
C2	11.8 ± 0.6	12.6 ± 0.1	13.2 ± 0.6	14.1 ± 0.5	**12.925^{c}**	1.55 ± 0.1	1.5 ± 0.1	1.36 ± 0.2	1.25 ± 0.01	**1.41^{bc}**
C3	11.9 ± 0.5	12.5 ± 0.2	12.9 ± 0.5	13.2 ± 0.8	**12.625 ^{cd}**	1.65 ± 0.2	1.45 ± 0.02	1.33 ± 0.01	1.24 ± 0.03	**1.41^{bc}**
C4	12.2 ± 0.4	12.5 ± 0.6	12.7 ± 0.8	13 ± 0.4	**12.6 ^{cd}**	1.72 ± 0.3	1.46 ± 0.2	1.36 ± 0.0	1.2 ± 0.01	**1.43^{b}**
C5	13 ± 0.6	13.5 ± 0.4	14 ± 0.5	14.9 ± 0.6	**13.85^{a}**	1.79 ± 0.1	1.55 ± 0.3	1.39 ± 0.01	1.1 ± 0.06	**1.45^{b}**
Mean	**12D**	**12.81C**	**13.35B**	**14.06A**		**1.58A**	**1.46B**	**1.40BC**	**1.31C**	

C1, KPI; C2, AG; C3, KPI/AG 0.5%; C4, KPI/AG/AgNPs 2%; C5 KPI/AG/AgNPs 1%. Total soluble soilds (TSS).

protects the liver tissue. It prevents it from fracturing and releasing these enzymes from the cytoplasm; additionally, it lowers ALT and AST and promotes the recovery of hepatocyte functions (Saleh et al., 2022). Malondialdehyde profoundly damages cell membranes, changing their structure and function (Nair and Nair, 2013; Saenthaweesuk et al., 2017; Said et al., 2019). MDA formation and buildup can lead to oxidative processes, inhibition, and cytotoxicity. Kumar et al. (2020) found that all broiler-fed diet serum biochemical parameters supplemented with AgNPs 50 μg/mL were in the normal ranges.

ROS can harm cells by oxidizing key biological components like membrane lipids, proteins, and DNA (Burri et al., 2017; Said et al., 2019). The mechanism of action of PPAgNPs was investigated because the phenolic compounds in the pomegranate wastes were potent anti-oxidants that positively influenced the lipid profile, according to the study's results (Alowaiesh et al., 2023); additionally silver nanoparticles decreased the programmed cell death caused by TNF-α because of the anti-inflammatory effect of AgNPs (Abdellatif et al., 2022); therefore, we recommended using PPAgNPs concentrations as a safe combinatory

Table 5
Changes in antioxidant activity of fruit juice during cold storage of 15, 30, 45, and 60 days.

Treatments	AA (%)				Mean
Storage (days)	15d	30d	45d	60d	
Control	75 ± 0.2	69 ± 0.6	58 ± 0.3	49 ± 0.2	**62^{d}**
C1	80 ± 0.3	72 ± 0.1	61 ± 0.1	52 ± 0.3	**66^{c}**
C2	82 ± 0.5	75 ± 0.2	66 ± 0.6	58 ± 0.4	**70^{bc}**
C3	86 ± 0.6	79 ± 0.6	69 ± 0.9	61 ± 0.6	**73^{b}**
C4	88 ± 0.5	81 ± 0.5	72 ± 0.1	66 ± 0.3	**76^{ab}**
C5	90 ± 0.3	82 ± 0.8	78 ± 0.4	72 ± 0.2	**80^{a}**
Mean	**83A**	**76B**	**67C**	**59D**	

C1, KPI; C2, AG; C3, KPI/AG 0.5 %; C4, KPI/AG/AgNPs 2 %; C5 KPI/AG/AgNPs 1 %. Data are presented mean ± SD. Antioxidant activity (AA).

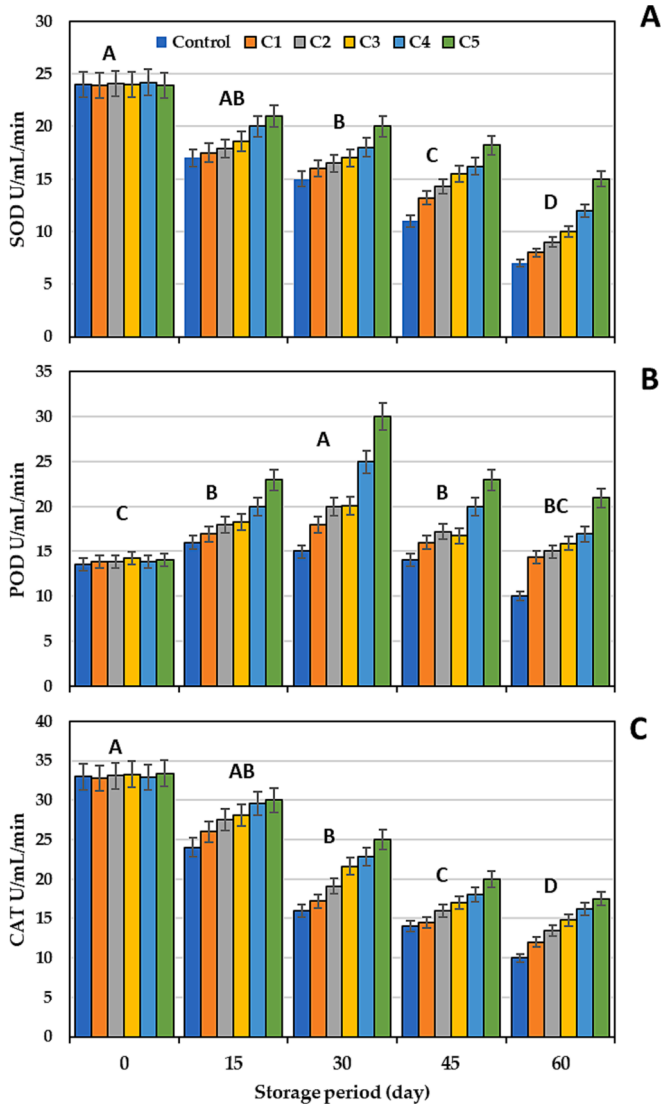

Fig. 9. The antioxidant enzymes content in Mandarin rind during cold storage of 0, 15, 30, 45, and 60 days and different coating treatments (A) sodium dismutase activity, (B) Peroxidase activity, and (C) Catalase activity. C1, KPI; C2, AG; C3, KPI/AG 0.5 %; C4, KPI/AG/AgNPs 2 %; C5 KPI/AG/AgNPs 1 %. Data presented mean ± SD. A-D uppercase letters above columns indicate signfcant differences.

treatment correlating with Kumar et al. (2020).

Because of the distinct properties of silver nanoparticles, they are included in a coating to ban the postharvest changes in mandarin fruit for 60 days; monitoring the physiochemical changes; the increase in TSS is attributable to the decay of polysaccharides into simple sugars during metabolic processes (Parven et al., 2020). Khorram et al. (2017) observed increasing TSS and TA in Arabic gum-coated mandarin fruit. Conversely, the obtained results noticed decreasing TA in coated fruits because of reducing the WVP and respiration rate.

The increase in phenolic and flavonoid contents in coated fruits because the coating acts as a barrier against oxygen reduces ROS and PPO activity that degraded the phenolic compounds (Adetoro et al., 2020). On the other hand, the active ingredients in AgNPs other than KPI strengthen the antioxidant activity of the Arabic gum coating (La et al., 2021).

Malondialdehyde is decreased by limiting respiration, and the activity of antioxidant enzymes like catalase, peroxidase, and superoxide dismutase are preserved by adding hairy fig to a chitosan-based coating (POD) (Chen et al., 2018). Peroxidase can regain its activity in stored foods and degrades raw and processed fruit's color, texture, and flavor (He et al., 2020). Our results are in agreement with Ali et al. (2021). POD's sensitivity to light and temperature may be the cause of its reduction after 30 days. Peroxidase activity in catalase catalyses the conversion of H_2O_2 into H_2O and O_2, preventing the accumulation of harmful levels of H2O2 brought on by metabolic processes (Amoako et al., 2015).

Fresh fruit suffers severe cellular damage from reactive oxygen species (ROS) during postharvest storage of horticulture crops; as a result, antioxidant defence enzymes have been shown to remove elements causing fruit cell membrane disintegration (Meitha et al., 2020). According to (Ma et al., 2021), lipid peroxidation is adverse to pulp cells. Consequently, using functional coatings can be advantageous for avoiding the formation of unsaturated fatty acids. Antioxidant activity is produced by a variety of non-enzymatic antioxidants as well as enzymatic defensive mechanisms like SOD, CAT, and POD. Fruits defend themselves from oxidative stress-related harm caused by ROS (Kapoor et al., 2019).

The shelf life of coated fruits is increased by edible coatings like Arabic gum, which keep less antioxidant enzyme activity and shield fruit tissues from active oxygen (Ali et al., 2021). Therefore, it may be speculated that KPI/AG/AgNPs 1 % regulated the Vermont mandarin fruit's oxygen exposure, reducing H_2O_2 buildup and delaying the fruit's senescence.

5. Conclusion

Valorizing food waste is a global trend. In this study, we valorize polyphenolic-rich pomegranate wastes by producing functional green silver nanoparticles with medical applications. The PPAgNPs have high phenolic content; therefore, they have potent activities, i.e., antioxidant, antimicrobial, antiviral, and anticancer activities. The studied concentrations of PPAgNPs were safe, influencing the normal biochemical and histological results of liver and kidney functions of rats. Because of the antioxidant and antimicrobial properties of PPAgNPs, we can safely use them to maintain the quality of citrus fruit stored at cold storage for an extended period.

Declaration of competing interest

The authors declare that they have no known competing financial interests or personal relationships that could have appeared to influence the work reported in this paper.

Acknowledgment

The researchers thank the Deanship of Scientific Research, Taif University, for funding this work.

References

Abdellatif, A., Osman, S., Alsharidah, M., Al Rugaie, O., Faris, T., Alqasoumi, A., Mousa, A., Bouazzaoui, A., 2022. Green synthesis of silver nanoparticles reduced with *Trigonella foenumgraecum* and their effect on tumor necrosis factor-α in MCF7 cells. Eur. Rev. Med. Pharmacol. Sci. 26, 5529–5539. https://doi.org/10.26355/eurrev_202208_29424.

Abdel-Raouf, N., Al-Enazi, N.M., Ibraheem, I.B., 2017. Green biosynthesis of gold nanoparticles using *Galaxaura elongata* and characterization of their antibacterial activity. Arab. J. Chem. 10, S3029–S3039. https://doi.org/10.1016/j.arabjc.2013.11.044.

Abdelsattar, A.S., Nofal, R., Makky, S., Safwat, A., Taha, A., El-Shibiny, A., 2021. The synergistic effect of biosynthesized silver nanoparticles and phage zcse2 as a novel approach to combat multidrug-resistant *Salmonella enterica*. Antibiotics 10 (6), 678. https://doi.org/10.3390/antibiotics10060678.

Adetoro, A.O., Opara, U.L., Fawole, O.A., 2020. Effect of blanching on enzyme inactivation, physicochemical attributes and antioxidant capacity of hot-air dried pomegranate (*Punica granatum* L.) arils (cv. wonderful). Processes 9 (1), 25. https://doi.org/10.3390/pr9010025.

Adje, F., Lozano, Y.F., Meudec, E., Lozano, P., Adima, A., N'zi, G.A., Gaydou, E.M., 2008. Anthocyanin characterization of pilot plant water extracts of *Delonix regia* flowers. Molecules 13, 1238-1245. https://doi.org/10.3390/molecules13061238.

Ahmad, S.S., Yousuf, O., Islam, R.U., Younis, K., 2021. Silver nanoparticles as an active packaging ingredient and its toxicity. Packag. Technol. Sci. 34, 653–663. https://doi.org/10.1002/pts.2603.

Alagawany, M., Qattan, S.Y., Attia, Y.A., El-Saadony, M.T., Elnesr, S.S., Mahmoud, M.A., Reda, F.M., 2021. Use of chemical nano-selenium as an antibacterial and antifungal agent in quail diets and its effect on growth, carcasses, antioxidant, immunity and caecal microbes. Animals 11 (11), 3027. https://doi.org/10.3390/ani11113027.

Ali, S., Anjum, M.A., Ejaz, S., Hussain, S., Ercisli, S., Saleem, M.S., Sardar, H., 2021. Carboxymethyl cellulose coating delays chilling injury development and maintains eating quality of 'Kinnow'mandarin fruits during low temperature storage. Int. J. Biol. Macromol. 168, 77–85. https://doi.org/10.1016/j.ijbiomac.2020.12.028.

Alowaiesh, B.F., Alhaithloul, H.A.S., Saad, A.M., Hassanin, A.A., 2023. Green Biogenic of silver nanoparticles using polyphenolic extract of olive leaf wastes with focus on their anticancer and antimicrobial activities. Plants 12 (6), 1410. https://doi.org/10.3390/plants12061410.

Alsubhi, N.H., Al-Quwaie, D.A., Alrefaei, G.I., Alharbi, M., Binothman, N., Aljadani, M., Qahl, S.H., Jaber, F.A., Huwaikem, M., Sheikh, H.M., 2022. Pomegranate pomace extract with antioxidant, anticancer, antimicrobial, and antiviral activity enhances the quality of strawberry-yogurt smoothie. Bioengineering 9 (12), 735. https://doi.org/10.3390/bioengineering9120735.

Amoako, S., Yahaya, A., Sarfo, J.K., 2015. Catalase activity of cassava (*Manihot esculenta*) plant under African cassava mosaic virus infection in *Cape coast*, Ghana. Afr. J. Biotechnol. 14 (14), 1201–1206. https://doi.org/10.5897/AJB2014.13864.

AOAC, 2012. Official Methods of Analysis of AOAC International. 19th edn. Washington, DC: AOAC.

Ashour, E.A., El-Hack, M.E.A., Shafi, M.E., Alghamdi, W.Y., Taha, A.E., Swelum, A.A., Tufarelli, V., Mulla, Z.S., El-Ghareeb, W.R., El-Saadony, M.T., 2020. Impacts of green coffee powder supplementation on growth performance, carcass characteristics, blood indices, meat quality and gut microbial load in broilers. Agriculture 10 (10), 457. https://doi.org/10.3390/agriculture10100457.

Attallah, N.G., Elekhnawy, E., Negm, W.A., Hussein, I.A., Mokhtar, F.A., Al-Fakhrany, O. M., 2022. *In vivo* and *in vitro* antimicrobial activity of biogenic silver nanoparticles against *Staphylococcus aureus* clinical isolates. Pharmaceuticals 15 (2), 194. https://doi.org/10.3390/ph15020194.

Attard, E., 2013. A rapid microtitre plate Folin-Ciocalteu method for the assessment of polyphenols. Open Life Sci. 8 (1), 48–53. https://doi.org/10.2478/s11535-012-0107-3.

Betts, J.W., Hornsey, M., La Ragione, R.M., 2018. Novel antibacterials: alternatives to traditional antibiotics. Adv. Microb. Physiol. 37, 123–169. https://doi.org/10.1016/bs.ampbs.2018.06.001.

Bhan, C., Asrey, R., Meena, N.K., Rudra, S.G., Chawla, G., Kumar, R., Kumar, R., 2022. Guar gum and chitosan-based composite edible coating extends the shelf life and preserves the bioactive compounds in stored Kinnow fruits. Int. J. Biol. Macromol. 222, 2922–2935. https://doi.org/10.1016/j.ijbiomac.2022.10.068.

Burri, S.C., Ekholm, A., Håkansson, Å., Tornberg, E., Rumpunen, K., 2017. Antioxidant capacity and major phenol compounds of horticultural plant materials not usually used. J. Funct. Foods 38, 119–127. https://doi.org/10.1016/j.jff.2017.09.003.

Chavan, P., Lata, K., Kaur, T., Jambrak, A.R., Sharma, S., Roy, S., Sinhmar, A., Thory, R., Singh, G.P., Aayush, K., 2023. Recent advances in the preservation of postharvest fruits using edible films and coatings: A comprehensive review. Food Chem. 418, 135916 https://doi.org/10.1016/j.foodchem.2023.135916.

Chen, C., Cai, N., Chen, J., Peng, X., Wan, C., 2018. Chitosan-based coating enriched with hairy fig (*Ficus hirta* Vahl.) fruit extract for "Newhall" navel orange preservation. Coatings 8 (12), 445. https://doi.org/10.3390/coatings8120445.

Chowdhury, N.N., Islam, M.N., Jafrin, R., Rauf, A., Khalil, A.A., Emran, T.B., Aljohani, A. S., Alhumaydhi, F.A., Lorenzo, J.M., Shariati, M.A., 2022. Natural plant products as effective alternatives to synthetic chemicals for postharvest fruit storage management. Crit. Rev. Food Sci. Nutr. 25, 1–19. https://doi.org/10.1080/10408398.2022.2079112.

Chung, I.-M., Rajakumar, G., Thiruvengadam, M., 2018. Effect of silver nanoparticles on phenolic compounds production and biological activities in hairy root cultures of *Cucumis anguria*. Acta Biol. Hung. 69 (1), 97–109. https://doi.org/10.1556/018.68.2018.1.8.

Dutta, T., Ghosh, N.N., Das, M., Adhikary, R., Mandal, V., Chattopadhyay, A.P., 2020. Green synthesis of antibacterial and antifungal silver nanoparticles using *Citrus limetta* peel extract: Experimental and theoretical studies. J. Environ. Chem. Eng. 8 (4), 104019 https://doi.org/10.1016/j.jece.2020.104019.

Ebada, D., Hefnawy, H.T., Gomaa, A., Alghamdi, A.M., Alharbi, A.A., Almuhayawi, M.S., Alharbi, M.T., Awad, A., Al Jaouni, S.K., Selim, S., 2023. Characterization of *Delonix regia* flowers' pigment and polysaccharides: evaluating their antibacterial, anticancer, and antioxidant activities and their application as a natural colorant and sweetener in beverages. Molecules 28 (7), 3243. https://doi.org/10.3390/molecules28073243.

Ehlers, J.L., 2016. Post-harvest rind pitting studies on 'Valencia'orange. Stellenbosch Univ ersity, Stellenbosch.

El-Ashry, R.M., El-Saadony, M.T., El-Sobki, A.E., El-Tahan, A.M., Al-Otaibi, S., El-Shehawi, A.M., Elshaer, N., 2022. Biological silicon nanoparticles maximize the efficiency of nematicides against biotic stress induced by *Meloidogyne incognita* in eggplant. Saudi J. Biol. Sci. 29 (2), 920–932. https://doi.org/10.1016/j.sjbs.2021.10.013.

El-Saadony, M.T., El-Wafai, N.A., El-Fattah, H.I.A., Mahgoub, S.A., 2019. Biosynthesis, optimization and characterization of silver nanoparticles using a soil isolate of *Bacillus pseudomycoides* MT32 and their antifungal activity against some pathogenic fungi. Adv. Anim. Vet. Sci. 7 (4), 238–249. https://doi.org/10.17582/journal.aavs/2019/7.4.238.249.

El-Saadony, M. T., Alkhatib, F. M., Alzahrani, S. O., Shafi, M. E., Abdel-Hamid, S. E., Taha, T. F., ... & Ahmed, N. H., 2021. Impact of mycogenic zinc nanoparticles on performance, behavior, immune response, and microbial load in *Oreochromis niloticus*. Saudi J. Biol. Sci. 29(2), 920-932. 28(8), 4592-4604. https://doi.org/10.1016/j.sjbs.2021.04.066.

Esmaeilzadeh Kenari, R., Razavi, R., 2022. Phenolic profile and antioxidant activity of free/bound phenolic compounds of sesame and properties of encapsulated nanoparticles in different wall materials. Food Sci. Nutr. 10, 525–535. https://doi.org/10.1002/fsn3.2712.

Ferreira, M.D., Neta, L.C.d.S., Brandão, G.C., Dos Santos, W.N.L., 2022. Evaluation of the antimicrobial activity of silver nanoparticles biosynthesized from the aqueous extract of *Schinus terebinthifolius* Raddi leaves. Appl. Biochem. Biotechnol. 70(3): 1001-1014. DOI: 10.1002/bab.2415.

Forner-Giner, M.Á., Ballesta-de los Santos, M., Melgarejo, P., Martínez-Nicolás, J.J., Melián-Navarro, A., Ruíz-Canales, A., Continella, A., Legua, P., 2023. Fruit quality and primary and secondary metabolites content in eight varieties of blood oranges. Agronomy 13(4), 1037. https://doi.org/10.3390/agronomy13041037.

Gallón, S.M.N., Alpaslan, E., Wang, M., Larese-Casanova, P., Londoño, M.E., Atehortúa, L., Pavón, J.J., Webster, T.J., 2019. Characterization and study of the antibacterial mechanisms of silver nanoparticles prepared with microalgal exopolysaccharides. Mater. Sci. Eng. 99, 685–695. https://doi.org/10.1016/j.msec.2019.01.134.

Gao, D., Yu, J., Dai, X., Tian, Y., Sun, J., Xu, X., Cai, X., 2023. Development and evaluation of an indirect enzyme-linked immunosorbent assay based on a recombinant SifA protein to detect *Salmonella* infection in poultry. Poult. Sci. 102 (4), 102513 https://doi.org/10.1016/j.psj.2023.102513.

Gherasim, O., Puiu, R.A., Bîrcă, A.C., Burduşel, A.-C., Grumezescu, A.M., 2020. An updated review on silver nanoparticles in biomedicine. Nanomaterials 10 (11), 2318. https://doi.org/10.3390/nano10112318.

Hasnaoui, N., Wathelet, B., Jiménez-Araujo, A., 2014. Valorization of pomegranate peel from 12 cultivars: Dietary fibre composition, antioxidant capacity and functional properties. Food Chem. 160, 196–203. https://doi.org/10.1016/j.foodchem.2014.03.089.

He, F., Zhao, L., Zheng, X., Abdelhai, M.H., Boateng, N.S., Zhang, X., Zhang, H., 2020. Investigating the effect of methyl jasmonate on the biocontrol activity of *Meyerozyma guilliermondii* against blue mold decay of apples and the possible mechanisms involved. Physiol. Mol. Plant Pathol. 109, 101454 https://doi.org/10.1016/j.pmpp.2019.101454.

Herald, T.J., Gadgil, P., Tilley, M., 2012. High-throughput micro plate assays for screening flavonoid content and DPPH-scavenging activity in sorghum bran and flour. J. Sci. Food Agric. 92 (11), 2326–2331. https://doi.org/10.1002/jsfa.5633.

Hussein, Z., Fawole, O.A., Opara, U.L., 2019. Determination of physical, biochemical and microstructural changes in impact-bruise damaged pomegranate fruit. J. Food Meas. Charact. 13, 2177–2189. https://doi.org/10.1007/s11694-019-00138-z.

Jafarzadeh, S., Nooshkam, M., Zargar, M., Garavand, F., Ghosh, S., Hadidi, M., Forough, M., 2023. Green synthesis of nanomaterials for smart biopolymer packaging: challenges and outlooks. J. Nanostruct. Chem. 1–24 https://doi.org/10.1007/s40097-023-00527-3.

Jia, N., Kong, B., Liu, Q., Diao, X., Xia, X., 2012. Antioxidant activity of black currant (*Ribes nigrum* L.) extract and its inhibitory effect on lipid and protein oxidation of pork patties during chilled storage. Meat Sci. 91 (4), 533–539. https://doi.org/10.1016/j.meatsci.2012.03.010.

Kapoor, D., Singh, S., Kumar, V., Romero, R., Prasad, R., Singh, J., 2019. Antioxidant enzymes regulation in plants in reference to reactive oxygen species (ROS) and reactive nitrogen species (RNS). Plant Gene 19, 100182. https://doi.org/10.1016/j.plgene.2019.100182.

Kemala, P., Idroes, R., Khairan, K., Ramli, M., Jalil, Z., Idroes, G.M., Tallei, T.E., Helwani, Z., Safitri, E., Iqhrammullah, M., Nasution, R., 2022. Green synthesis and antimicrobial activities of silver nanoparticles using *Calotropis gigantea* from Ie Seu-Um geothermal area, aceh province, Indonesia. Molecules 27 (16), 5310. https://doi.org/10.3390/molecules27165310.

Khairy, A.M., Tohamy, M.R., Zayed, M.A., Mahmoud, S.F., El-Tahan, A.M., El-Saadony, M.T., Mesiha, P.K., 2022. Eco-friendly application of nano-chitosan for

controlling potato and tomato bacterial wilt. Saudi J. Biol. Sci. 29 (4), 2199–2209. https://doi.org/10.1016/j.sjbs.2021.11.041.
Khorram, F., Ramezanian, A., Hosseini, S.M.H., 2017. Effect of different edible coatings on postharvest quality of 'Kinnow' mandarin. J. Food Meas. Charact. 11 (4), 1827–1833. https://doi.org/10.1007/s11694-017-9564-8.
Ko, K., Dadmohammadi, Y., Abbaspourrad, A., 2021. Nutritional and bioactive components of pomegranate waste used in food and cosmetic applications: A review. Foods 10 (3), 657. https://doi.org/10.3390/foods10030657.
Kovács, D., Igaz, N., Gopisetty, M.K., Kiricsi, M., 2022. Cancer therapy by silver nanoparticles: fiction or reality? Int. J. Mol. Sci. 23 (2), 839. https://doi.org/10.3390/ijms23020839.
Kumar, I., Bhattacharya, J., Das, B.K., Lahiri, P., 2020. Growth, serum biochemical, and histopathological responses of broilers administered with silver nanoparticles as a drinking water disinfectant. 3 Biotech 10(3), 94. DOI: 10.1007/s13205-020-2101-1.
La, D.D., Nguyen-Tri, P., Le, K.H., Nguyen, P.T., Nguyen, M.-D.-B., Vo, A.T., Nguyen, M. T., Chang, S.W., Tran, L.D., Chung, W.J., 2021. Effects of antibacterial ZnO nanoparticles on the performance of a chitosan/gum arabic edible coating for post-harvest banana preservation. Prog. Org. Coat. 151, 106057 https://doi.org/10.1016/j.porgcoat.2020.106057.
Ma, J., Zhou, Z., Li, K., Li, K., Liu, L., Zhang, W., Xu, J., Tu, X., Du, L., Zhang, H., 2021. Novel edible coating based on shellac and tannic acid for prolonging postharvest shelf life and improving overall quality of mango. Food Chem. 354, 129510 https://doi.org/10.1016/j.foodchem.2021.129510.
Manzoor, A., Dar, A.H., Pandey, V.K., Shams, R., Khan, S., Panesar, P.S., Kennedy, J.F., Fayaz, U., Khan, S.A., 2022. Recent insights into polysaccharide-based hydrogels and their potential applications in food sector: A review. Int. J. Biol. Macromol. 213, 987–1006. https://doi.org/10.1016/j.ijbiomac.2022.06.044.
Mawed, S.A., Marini, C., Alagawany, M., Farag, M.R., Reda, R.M., El-Saadony, M.T., El-Nagar, W.G., 2022. Zinc oxide nanoparticles (ZnO-NPs) suppress fertility by activating autophagy, apoptosis, and oxidative stress in the developing oocytes of female zebrafish. Antioxidants 11 (8), 1567. https://doi.org/10.3390/antiox11081567.
Mazen, N.F., Saleh, E.Z., Mahmoud, A.A., Shaalan, A.A., 2017. Histological and immunohistochemical study on the potential toxicity of sliver nanoparticles on the structure of the spleen in adult male albino rats, Egypt. J. Histol. 40, 374–387. https://doi.org/10.21608/EJH.2017.4662.
Meitha, K., Pramesti, Y., Suhandono, S., 2020. Reactive oxygen species and antioxidants in postharvest vegetables and fruits. Int. J. Food Sci. 10 (2020), 1–11. https://doi.org/10.1155/2020/8817778.
Morris, D., Ansar, M., Speshock, J., Ivanciuc, T., Qu, Y., Casola, A., Garofalo, R.P., 2019. Antiviral and immunomodulatory activity of silver nanoparticles in experimental RSV infection. Viruses 11 (8), 732. https://doi.org/10.3390/v11080732.
Nair, G.G., Nair, C.K.K., 2013. Radioprotective effects of gallic acid in mice. BioMed Res. Int. 2013, 953079 https://doi.org/10.1155/2013/953079.
Natan, M., Banin, E., 2017. From nano to micro: using nanotechnology to combat microorganisms and their multidrug resistance. FEMS Microbiol. Rev. 41, 302–322. https://doi.org/10.1093/femsre/fux003.
Parven, A., Sarker, M.R., Megharaj, M., Meftaul, I.M., 2020. Prolonging the shelf life of Papaya (*Carica papaya* L.) using Aloe vera gel at ambient temperature. Sci. Hortic. 265, 109228 https://doi.org/10.1016/j.scienta.2020.109228.
Ranjah, M.A., Waseem, M., Taj, F., Ashraf, I., 2019. Lemongrass: A useful ingredient for functional foods. Int. J. Food Allied Sci. 4 (2), 11–19.
Ratan, Z.A., Mashrur, F.R., Chhoan, A.P., Shahriar, S.M., Haidere, M.F., Runa, N.J., Kim, S., Kweon, D.-H., Hosseinzadeh, H., Cho, J.Y., 2021. Silver nanoparticles as potential antiviral agents. Pharmaceutics 13 (12), 2034. https://doi.org/10.3390/pharmaceutics13122034.
Repetto, G., Del Peso, A., Zurita, J.L., 2008. Neutral red uptake assay for the estimation of cell viability/cytotoxicity. Nat. Protoc 3, 1125–1131. https://doi.org/10.1038/nprot.2008.75.
Saad, A.M., El-Saadony, M.T., El-Tahan, A.M., Sayed, S., Moustafa, M.A., Taha, A.E., Taha, T.F., Ramadan, M.M., 2021a. Polyphenolic extracts from pomegranate and watermelon wastes as substrate to fabricate sustainable silver nanoparticles with larvicidal effect against *Spodoptera littoralis*. Saudi J. Biol. Sci. 28 (10), 5674–5683. https://doi.org/10.1016/j.sjbs.2021.06.011.
Saad, A.M., Mohamed, A.S., El-Saadony, M.T., Sitohy, M.Z., 2021b. Palatable functional cucumber juices supplemented with polyphenols-rich herbal extracts. LWT - Food Sci. Technol. 148, 111668 https://doi.org/10.1016/j.lwt.2021.111668.
Saad, A.M., Sitohy, M.Z., Ahmed, A.I., Rabie, N.A., Amin, S.A., Aboelenin, S.M., Soliman, M.M., El-Saadony, M.T., 2021c. Biochemical and functional characterization of kidney bean protein alcalase-hydrolysates and their preservative action on stored chicken meat. Molecules 26 (15), 4690. https://doi.org/10.3390/molecules26154690.
Sabra, M.A., Alaidaroos, B.A., Jastaniah, S.D., Heflish, A.I., Ghareeb, R.Y., Mackled, M.I., Conte-Junior, C.A., 2022. Comparative effect of commercially available nanoparticles on soil bacterial community and "*Botrytis fabae*" caused brown spot: *In vitro* and *in vivo* experiment. Front. Microbiol. 13, 934031 https://doi.org/10.3389/fmicb.2022.934031.
Saenthaweesuk, S., Munkong, N., Parklak, W., Thaeomor, A., Chaisakul, J., Somparn, N., 2017. Hepatoprotective and antioxidant effects of *Cymbopogon citratus* Stapf (Lemon grass) extract in paracetamolinduced hepatotoxicity in rats. Trop. J. Pharm. Res. 16, 101–107. https://doi.org/10.4314/tjpr.v16i1.13.
Said, A.M., Atwa, S.A., Khalifa, O.A., 2019. Ameliorating effect of gum arabic and lemongrass on chronic kidney disease induced experimentally in rats. Bull. Natl. Res. Cent. 43, 1–8. https://doi.org/10.1186/s42269-019-0086-x.
Saleh, S.R., Manaa, A., Sheta, E., Ghareeb, D.A., Abd-Elmonem, N.M., 2022. The synergetic effect of egyptian *Portulaca oleracea* L. (Purslane) and *Cichorium intybus* L. (Chicory) extracts against glucocorticoid-induced testicular toxicity in rats through attenuation of oxidative reactions and autophagy. Antioxidants 11 (7), 1272. https://doi.org/10.3390/antiox11071272.
Shejawal, K.P., Randive, D.S., Bhinge, S.D., Bhutkar, M.A., Todkar, S.S., Mulla, A.S., Jadhav, N.R., 2021. Green synthesis of silver, iron and gold nanoparticles of lycopene extracted from tomato: their characterization and cytotoxicity against COLO320DM, HT29 and Hella cell. J. Mater Sci. Mater. Med. 32, 1–12. https://doi.org/10.1007/s10856-021-06489-8.
Simbine, E.O., Rodrigues, L.d.C., Lapa-Guimaraes, J., Kamimura, E.S., Corassin, C.H., Oliveira, C.A.F.d., 2019. Application of silver nanoparticles in food packages: a review. Food Sci. Technol. 39(4), 793-802. https://doi.org/10.1590/fst.36318.
Sreelekha, E., George, B., Shyam, A., Sajina, N., Mathew, B., 2021. A Comparative study on the synthesis, characterization, and antioxidant activity of green and chemically synthesized silver nanoparticles. BioNanoScience 11, 489–496. https://doi.org/10.1007/s12668-021-00824-7.
Srikhao, N., Ounkaew, A., Srichiangsa, N., Phanthanawiboon, S., Boonmars, T., Artchayasawat, A., Theerakulpisut, S., Okhawilai, M., Kasemsiri, P., 2022. Green-synthesized silver nanoparticle coating on paper for antibacterial and antiviral applications. Polym. Bull. 17, 1–18. https://doi.org/10.1007/s00289-022-04530-6.
Suvarna, K.S., Layton, C., Bancroft, J.D., 2018. Bancroft's theory and practice of histological techniques E-Book. 8th Edition Elsevier health sciences.
Wang, C., Gong, C., Qin, Y., Hu, Y., Jiao, A., Jin, Z., Qiu, C., Wang, J., 2022. Bioactive and functional biodegradable packaging films reinforced with nanoparticles. J. Food Eng. 312, 110752 https://doi.org/10.1016/j.jfoodeng.2021.110752.
Yadav, A., Kumar, N., Upadhyay, A., Sethi, S., Singh, A., 2022. Edible coating as postharvest management strategy for shelf-life extension of fresh tomato (*Solanum lycopersicum* L.): An overview. J. Food Sci. 87, 2256–2290. https://doi.org/10.1111/1750-3841.16145.
Yadav, P., Yadav, R., Jain, S., Vaidya, A., 2021. Caspase-3: A primary target for natural and synthetic compounds for cancer therapy. Chem. Biol. Drug. Des. 98, 144–165. https://doi.org/10.1111/cbdd.13860.
Yehia, N., AbdelSabour, M.A., Erfan, A.M., Ali, Z.M., Soliman, R.A., Samy, A., Ahmed, K. A., 2022. Selenium nanoparticles enhance the efficacy of homologous vaccine against the highly pathogenic avian influenza H5N1 virus in chickens. Saudi J. Biol. Sci. 29 (4), 2095–2111. https://doi.org/10.1016/j.sjbs.2021.11.051.
Zacarias, L., Cronje, P.J., Palou, L., 2020. Postharvest technology of citrus fruits, the genus citrus. Elsevier 421–446. https://doi.org/10.1016/B978-0-12-812163-4.00021-8.